Preprints (www.preprints.org) | NOT PEER-REVIEWED | Posted: 12 October 2022 doi:10.20944/preprints202210.0167.v1

Trivariate joint distribution modelling of compound events using the nonparametric D-vine copula developed based on Bernstein and Beta kernel copula density framework

Shahid Latif [1*] and Slobodan P. Simonovic [1]

[1] Department of Civil and Environmental Engineering, Western University, London, ON N6A 5B8, Canada; macet.shahid@gmail.com

* Correspondence: macet.shahid@gmail.com

Abstract: Low-lying coastal communities are often threatened by compound flooding (CF), which can be determined through the joint occurrence of storm surges, rainfall and river discharge either successively or in close succession. The trivariate distribution can demonstrate the risk of the compound phenomenon more realistically rather than considering each contributing factor independently or in a pairwise dependency. Recently vine copula has been recognized as the highly flexible approach to constructing a higher dimensional joint density framework. In such construction, parametric class copula with parametric univariate marginal distributions is often involved. Such incorporation can lack flexibility due to parametric functions with prior distribution assumptions about their univariate marginal and/or copula joint density. This study introduces the vine copula approach in a nonparametric setting by introducing Bernstein and Beta kernel copula density in establishing trivariate flood dependence. The proposed model is applied to 46 years of flood characteristics collected on the west coast of Canada. The univariate flood marginal distribution is modelled using nonparametric kernel density estimation (KDE). The 2-D Bernstein estimator and Beta kernel copulas estimator are tested independently in capturing pairwise dependencies to establish D-vine structure in a stage-wise nesting approach in three alternative ways, each by permutating the location of the conditioning variable. The best-fitted vine structure is selected using goodness-of-fit (GOF) test statistics. The performance of the nonparametric vine approach is also compared with the vine constructed in the parametric and semiparametric fitting procedure. Investigation reveals that the D-vine constructed using Bernstein copula with normal KDE marginals nonparametrically performed well in capturing dependence of the compound events. Finally, the derived nonparametric model is used in the estimation of trivariate OR- and AND-joint return periods, further employed in estimating failure probability (FP) statistics. The trivariate return periods for the AND-joint case are higher than for the OR-joint case for the same flood combination. Also, the trivariate flood hazard results in a high-value FP than bivariate and univariate events. Ignoring the trivariate dependence could result in the underestimation of FP

Keywords: compound flooding; D-vine copula; trivariate joint analysis; Bernstein estimator; Beta kernel estimator; parametric copulas; kernel density estimation; return periods

1. Introduction

A compound event (CE) is a multidimensional phenomenon that can be defined by the joint probability occurrence of two or more extreme or non-extreme events, which may not be dangerous or devastating if considered individually [1-3]. However, CE can be severe consequences if their underlying variables co-occur or are in close succession. On the global scale, the flooding events in low-lying coastal cities or the risk of extreme compound phenomena have already been recorded and outlined in the previous literature [4-6 and references therein]. The climate-changing scenario has already triggered a rising coastal water level called sea level rise (SLR) and increased the frequency and severity of flooding that threatens coastal communities worldwide [7-9]. The coastal region flooding can be significantly

 doi:10.20944/preprints202210.0167.v1

defined and estimated by combining the multiple driving forces, such as storm surge (oceanographic), rainfall (or pluvial flooding) and river discharge (or fluvial flooding). These events can be interlinked through a common forcing mechanism such as tropical or extra-tropical cyclones (or low atmospheric pressure scenario). On the other side, these source variables do not always need to co-occur. For example, when a storm enters from the coast of land towards inland, it may take 1 or 2 days or more to have high rainfall after the storm events, leading to heavy streamflow discharge. Among the different coastal flood drivers, a storm surge event is often considered a significant flood-driving agent [10]. When combined with rainfall (e.g., [2]) or with high river discharge (e.g., [9]), it can result in a devastating situation.

Different mathematical or statistical frameworks are often pointed out in the demonstration of the compound extreme or flooding phenomenon but still can lack a consistent or robust approach. The traditional statistical evaluation of the compound events is usually a multivariate framework that observes the number of extreme joint episodes by targeting the most justifiable flood-driving factors. For instance, the study made by Coles [11], Coles et al., [12] Svensson and Jones [13], Cooley et al. [14], Zheng et al. [15] and Zheng et al. [16] and references therein. In reality, the validity of the univariate probability or frequency analysis (and return periods) would be questionable. Due to the multidimensional behaviour, it must demand an efficient multivariate probability framework that can reduce the hydrologic risk much more efficiently than considering the probability distribution of each driving agent separately.

In recent studies, copula functions gained more popularity than traditional multivariate models and are recognized as highly flexible tools in the bivariate or multivariate joint distribution analysis of hydrometeorological observations (17-21 and references therein]. In the modelling of CE or flooding, the adequacy of different parametric class 2-D copulas is tested by targeting different contributing variables, for instance, between storm surge (or storm tide) and rainfall or between storm surge (or storm tide) and river discharge etc., [22-27 and references therein]. Such incorporations are limited to bivariate joint cases, employing 2-D parametric class copulas to observe pairwise joint dependency. However, the more realistic and practical flood risk can be obtained by compounding the joint distribution behaviour, including more relevant flood-driving agents (e.g., storm surge, rainfall, and river discharge) simultaneously instead of their pairwise dependency. For instance, tropical cyclones in the coastal region can trigger storm surges, rainfall, and possible high river discharge events simultaneously; thus, the complex mutual concurrency or interplay between them can exacerbate flooding in the coastal zones. Therefore, the risk of coastal flooding can be analyzed much more efficiently or in much better detail by considering the above triplet variable simultaneously instead of just considering bivariate joint dependency.

The application of the 3-D (or any higher dimension) copula in hydrometeorological modelling is minimal. Few previous works highlighted, for instance, asymmetric fully nested Archimedean copula [28-29]; Meta-elliptical Student's t copula [20]; Plackett copula [31]; Entropy copula [32]. All such framework has some statistical constraints and limitations when projected into a higher dimension, more variable. Such as, the 3-D symmetric Archimedean copula modelled the dependencies between multiple random variables by employing single-dependence parameters or generator functions, thus can not preserve all pairwise dependencies at the lower stages [31, 33]. Besides this, an asymmetric or fully nested Archimedean (FNA) copula can be much more reliable than a symmetric Archimedean structure. FNA can individually approximate each random attribute pair through multiple parametric joint asymmetric functions [34-36]. The faithful preservation of all the lower-level dependencies among the targeted variables is still challenging based on the FNA structure. This framework is only effective and practical when two

Preprints (www.preprints.org) | NOT PEER-REVIEWED | Posted: 12 October 2022 doi:10.20944/preprints202210.0167.v1

correlation structures are identical or near and lesser than the third correlation structure and only limited to a positive range [30]. Also, when considering more variables or an increase in dimension, the asymmetric FNA structure permits a narrow range of mutual dependencies [17]. Therefore, to alleviate all such statistical issues, the vine or pair-copula construction (PCC) approach is highly flexible and is a much more practical way of constructing any higher dimensional joint dependence by mixing multiple 2-D (bivariate) copulas in a stage-wise hierarchical nesting procedure [37-40 and references therein]. This approach to constructing a higher dimensional copula exhibits a conditional mixing procedure.

In CF modelling, Bevacqua et al. [41] introduced a 3-D vine copula for evaluating flooding events in Ravenna, Italy. In a recent study, Jane et al. [42] introduced the vine framework in the trivariate joint analysis of rainfall, oceanside water level and groundwater level observations in South Florida, USA. Besides the above two, other recent studies, for instance, Graler et al. [40]; Saghafian and Mehdikhani [43], Tosunoglu et al. [44], Latif and Mustafa [45] and references therein, often incorporated vine under parametric distribution settings, fitting the parametric class 2-D copulas with parametric marginal pdf in the parametric fitting procedure. Referred some previous literature, such as Silverman [46], Moon and Lall [47]; Sharma [48]; Kim et al. [49]; Karmakar and Simonovic [50] etc., it is revealed that the performance of nonparametric kernel density estimation (KDE) is much better than parametric family functions. Due to the absence of any prior distribution assumption about their marginals probability density function (PDF) type, KDE performed much more reliable, especially suited for multimodal or skewed random samples. However, the copula function eliminates the restriction to model any marginal distribution from the same family functions. On the other side, the subjective assumption of the joint PDF type of the fitted parametric copulas in the traditional vine distribution framework is not much more effective in approximating joint structure, which would be questionable. In other words, fixing the joint PDF of the dependence structure to any specific or predefined copula class must be lacking to fully acknowledge the flexibility of the copula fitted in the vine tree structure. Parametric copulas are frequently appeared because of their simplicity. However, another side, parameter estimation procedures of the fitted parametric models are time-consuming using standard statistical techniques, which might contribute to underestimating the actual joint probability density [51]. Rauf and Zeephongsekul [52] study claimed that it could lead to spurious inferences and be challenging if the underlying assumptions of the fitted parametric distribution are violated. Besides this, fitting an appropriate parametric copula could demand much attention and extra caution, which might bear the risk of uncertainty in their estimated joint exceedance values if an inappropriate dependence structure is selected.

To deal with all the above-raised issues, introducing the nonparametric copula density in the vine copula construction could be a better alternative where the 2-D copulas can adapt to any dependence structure without having any specific or fixed joint PDF form. To do this, the Bernstein copula estimator and Beta kernel copula density can be a good choice in modelling multivariate copula density in nonparametric settings (53-57 and references therein). In reality, the Bernstein copula can provide a higher consistency and lack boundary bias problems [58], resulting in a better estimation of the underlying dependence structure than empirical copulas estimate. Besides this, the performance of Beta kernel density is already proved by Rauf and Zeephongsekul [52] and Latif and Mustafa [21]. The nonparametric copula density gained more attention in economics but is rarely accepted in hydro-meteorological studies. Also, all the above nonparametric frameworks are often limited to bivariate cases.

The main contribution of the present work is the first to incorporate the Bernstein estimator and Beta kernel copula estimator in the nonparametric estimation of the 3-D vine copula density in the trivariate probability modelling of CF events. Both the above-mentioned nonparametric copula densities are tested in establishing the D-vine copula tree structure and in determining trivariate joint cumulative distribution functions (JCDF). This study also compared the performance of the semiparametric approach in the vine copula density, introducing parametric copulas with nonparametric marginal pdfs and the parametric approach in the vine copula with the proposed nonparametric density. The selected best-fitted model is employed in compounding the impact of storm surge, rainfall, and river discharge observations in assessing flood risk on the west coast of Canada. Our recent study is the first that incorporates the Bernstein estimator in flood modelling and confirms that this function performed well compared to Beta copula density in the bivariate dependence modelling of storm surge and rainfall events [59]. Our present study extends the previous bivariate approach by dealing with three variables, integrating the impact of river discharge events with storm surge and rainfall events in the risk of compound flooding (CF) events. Pirani and Najafi's [60] study already shows that the higher risk of compound extreme on Canada's west coasts is due to the joint impact of precipitation, extreme water level (also, storm surge events) and streamflow discharge. Also, west or Pacific Canada's coast experienced higher coastal instability because of the higher risk of coastal water levels [61].

This paper is organized into four sections. After the introduction, the required theoretical background of the nonparametric copula density and in development of the 3-D vine copula framework are discussed in section 2. Section 3 of this manuscript presents the application of the developed trivariate distribution framework to a case study in compounding the joint impact of rainfall, storm surge and river discharge events. This section comprises, for instance, modelling univariate marginal distribution via nonparametric KDE, constructing D-vine structure in the nonparametric fitting procedure via Bernstein and Beta copula estimator, and D-vine structure under the parametric fitting procedure and in the semiparametric settings. This section also compares the model adequacy and performance of all three developed D-vine structures in the trivariate CF dependence. Also, the best-fitted trivariate structure is employed in estimating primary joint return periods for both AND and OR-joint cases. Finally, section 4 provided the research summary and conclusions.

2. Methodology

2.1. Nonparametric copula density estimator

Figure 1 illustrates the methodological workflow used in this study. Firstly, compound flood variables' marginal distributions are modelled using the nonparametric kernel density estimation (KDE). The best-fitted parametric family distributions are adapted from our previous study (Latif and Simonovic 2022a), and their performance is compared with the selected KDE in the present study. The D-vine copula framework is developed under parametric, semiparametric, and nonparametric settings, and their performance is compared in describing the most parsimonious flood dependence. The nonparametric vine density comprises multiple 2-D copulas via the Bernstein and Beta kernel density with kernel density margins without having any prior assumption about their marginal pdf and joint density function. The parametric and semiparametric vine copula density defines through parametric class 2-D copulas (i.e., Archimedean and Extreme value) with parametric and nonparametric via KDE margins. The best-fitted trivariate structure is employed in the estimation of trivariate joint return periods for both OR-and AND-joint cases and is further employed in estimating failure probability (FP). In this study, the D-vine copula are developed for three different cases, each defined by permutating the location of the conditioning variable. For instance, in case 1, the river discharge event is a conditioning variable; in case 2, the storm surge event is a conditioning variable; in case 3, the rainfall event is a conditioning variable.

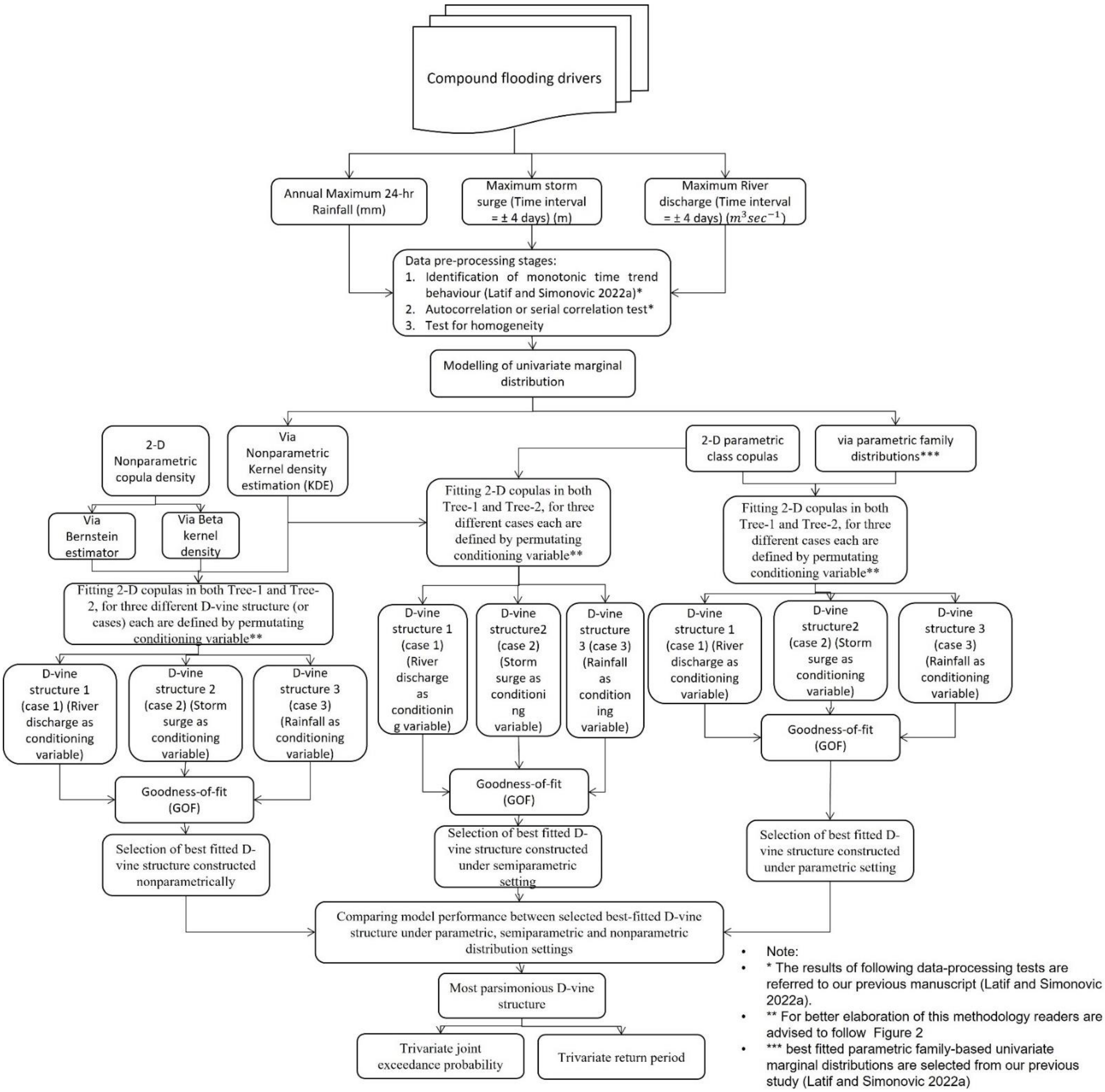

Figure 1: Workflow chart of the present study

 doi:10.20944/preprints202210.0167.v1

Mirror image modification, transformed kernels, boundary kernels etc., are a few examples of nonparametric approaches in joint density estimation [62-64]. This study introduces the Beta kernel copula and Bernstein copula estimator in developing the D-vine structure in the trivariate joint analysis of storm surge, rainfall and river discharge events on flood risk in the coastal regions. The Beta kernel copula density was discussed earlier by Brown and Chen [65], Harrell and Davis [53], and Chen [66], which is naturally free of boundary bias problems which often encountered in the standard kernel estimator. The consistency remains in the Beta kernel density if the actual density is unbounded at the boundary [67].

The 1-D Beta kernel density function for the given univariate variables, $A_1, A_2, \dots \dots . A_t$ is estimated by:

$$s_h(a) = \frac{1}{t}\sum_{i=1}^{t} K(A_i\, ,\ \frac{a}{h} + 1,\ \frac{1-a}{h} + 1) \tag{1}$$

where 'h' is the kernel bandwidth.

In the above Equation (1), the density of the Beta kernel function with parameters f and g is estimated by

$$K(a, f, g) = \frac{a^f (1-a)^g \Gamma(f)\Gamma(g)}{\Gamma(f+g)}, \qquad a \in [0,1] \tag{2}$$

According to Charpentier et al. [51], multiplying the Beta kernel densities can result in beta copula joint density known as Beta kernel copula at a point (a, b) as given below.

$$c_h(a, b) = \frac{1}{ph^2}\sum_{i=1}^{p} K(A_i\, ,\ \frac{a}{h} + 1,\ \frac{1-a}{h} + 1) \times K(B_i,\ \frac{b}{h} + 1,\ \frac{1-b}{h} + 1) \tag{3}$$

The bandwidth of Equation (3) is estimated by the rule of thumb (ROT) estimation procedure which is based on minimizing the asymptotic mean integrated squared error (AMISE) statistics. For this, Nagler [68] pointed out the applicability of the Frank copula as the reference copula. The ROT bandwidth estimation for the fitted 2-D Beta kernel estimator of Equation (3) is estimated by

$$h = \left(\frac{1}{8\pi}\frac{\varsigma(c)}{\xi(c)}\right)^{1/3} n^{-1/3} \tag{4}$$

where 'c' is assumed to be Frank copula in the above Equation (4)

On the other side, the efficacy of the Bernstein copula estimator is also tested and compared in constructing the D-vine structure together with Beta kernel density. Lorentz [69] highlighted that the Bernstein polynomial could be used to approximate any continuous functions within a range of [0,1]. Tenbush [70] constructed bivariate joint density using the Bernstein estimator. Approximation of nonparametric joint density using the Bernstein copula can provide higher consistency and lack boundary bias problems [55, 56, 71]. Also, it can better estimate the underlying mutual correlation and good approximation at an asymmetric and extreme dependency compared to an empirical copula approach [72].

Mathematically, n degree Bernstein polynomial is estimated by [56, 72]:

$$B(n, w, z) = \binom{n}{w} z^w (1-z)^{n-w} \tag{5}$$

In Equation (5), $w = 0,1,2, \dots \dots, n \in \mathbb{N}; 0 \le z \le 1$.

Now, if $X = (X_1, X_2)$ illustrates bivariate observations having uniform marginal distribution over $Y_i = \{0, 1, 2, \dots \dots \dots \dots, n_i\}$ with grid size $n_i \in \mathbb{N}$ and where $i = 1, 2$. Then,

$$y(w_1, w_2) = Y(\cap_{i=1}^{2}\{X_i = w_i\}), (w_1, w_2) \in [0,1]^2 \tag{6}$$

Hence, for the 2-D joint distribution case, the Bernstein copula density is estimated by.

$$c(x_1, x_2) = \sum_{w_1=0}^{n_1-1} \sum_{w_2=0}^{n_2-1} y(w_1, w_2) \prod_{i=1}^{2} n_i B(n_i - 1, w_i, x_i), \tag{7}$$

where $(x_1, x_2) \in [0,1]^2$.

2.2. *Univariate Kernel density estimation of flood margins*

Parametric class functions are often restricted to prior distributional assumptions about their univariate marginal pdfs. A nonparametric kernel density estimation (KDE) is already identified as much more robust and better performance in modelling the probability density of different hydrometeorological characteristics [47, 49, 73, 74 and references therein].

Mathematically, the 1-D kernel function can approximate probability density structure having the following statistical property

$$\int_{-\infty}^{+\infty} K(x)dx = 1 \tag{8}$$

Furthermore, the kernel function can be represented by a general function

$$K_o(x) = \frac{1}{o} K\left(\frac{x}{o}\right) \tag{9}$$

Where 'o' is the bandwidth of the fitted univariate kernel function.

By taking the average of Equation (9), the univariate kernel density estimator $\widehat{f_o}(x)$ of the probability density function is estimated by

$$\widehat{f_o}(x) = \frac{1}{po} \sum_{i=1}^{p} K_o\left(\frac{x - X_i}{o}\right) \tag{10}$$

Where 'p' is the observation counts. In fitting the kernel density to the given observational samples, selecting an appropriate way of estimating kernel bandwidth is often essential; otherwise, it may attribute to either over-smoothing or under or insufficient smoothing (also called rough smoothing). Readers are advised to follow Sharma et al. [48] and Jones et al. [76] for extended details about different statistical procedures in kernel bandwidth estimation. In our present analysis, the direct plug-in (DPI) method is used to estimate the bandwidth of the fitted kernel density [76-78]. Table 1 lists some kernel density functions which are used in this study.

Preprints (www.preprints.org) | NOT PEER-REVIEWED | Posted: 12 October 2022 doi:10.20944/preprints202210.0167.v1

Table 1: 1-D Kernel density estimation (KDE) tested in the modelling of flood marginals

SI no.	Kernel density estimation	K(x)
1	Normal	$=(2\pi)^{-1/2}e^{-(x^2)/2}$
2	Epanechnikov (or parabolic)	$= 0.75(1-x^2),\ \lvert X\rvert \leq 1$ = 0, otherwise
3	Biweight (or Quartic)	$= 0.9375(1-x^2)^2,\ \lvert x\rvert \leq 1$ $= 0$, otherwise
4	Triweight	$1.09375(1-x^2)^3,\ \lvert x\rvert \leq 1$ $= 0$, otherwise

2.3. D-vine copula structure in the trivariate modelling

The vine or pair-copula construction (pcc) is based on the decomposition of full multivariate density into a cascade of local blocks of the best-fitted 2-D copulas modelled between each random pair and their conditional and unconditional functions [37, 38]. Two famous decomposition steps in the vine framework, such as Canonical or C-vine and Drawable or D-vine [79, 80], where the D-vine structure is highly flexible, are accepted widely [39, 40, 81]. The traditional approach in the vine framework considered multiple 2-D parametric class copulae in the stagewise hierarchy. A few statistical constraints with parametric copula joint density are highlighted in section 1. Therefore, it could be problematic if the vine copula is constructed using the parametric class copulas. Because of this, the proposed methodology introduces and tests the efficacy of the nonparametric via Beta kernel copula density and Bernstein copula estimator individually in the 3-D vine simulation for the given CF variables. This study also compares the performance of the parametric and semiparametric approaches in the vine simulation, where both frameworks are defined through multiple 2-D parametric copulas. The univariate marginal distribution is modelled using the kernel density estimations (KDE) in both nonparametric and semiparametric, and parametric class distributions in the parametric vine approach.

Because of the involvement of three flood characteristics in characterizing CF events in our study, the present 3-D vine framework must demand three 2-D copulae and two tree levels, Tree 1 and Tree 2 (refer to Figure 2). For trivariate variables (A, B, C), the D-vine structure can be mathematically expressed as

$$\mathrm{f(a,b,c) = f(a).\,f(b|a) \cdot f(c|a,b)} \tag{11}$$

$$f(b|a) = \frac{f(a,b)}{f(a)} = c_{ab}\big(F(a), F(b)\big) \cdot f(b) \tag{12}$$

$$f(c|a,b) = {f(b,c|a)}\big/{f(b|a)} = c_{bc|a}(F(b|a), F(c|a)) \cdot c_{ac}(F(a), F(c)) \cdot f(c) \tag{13}$$

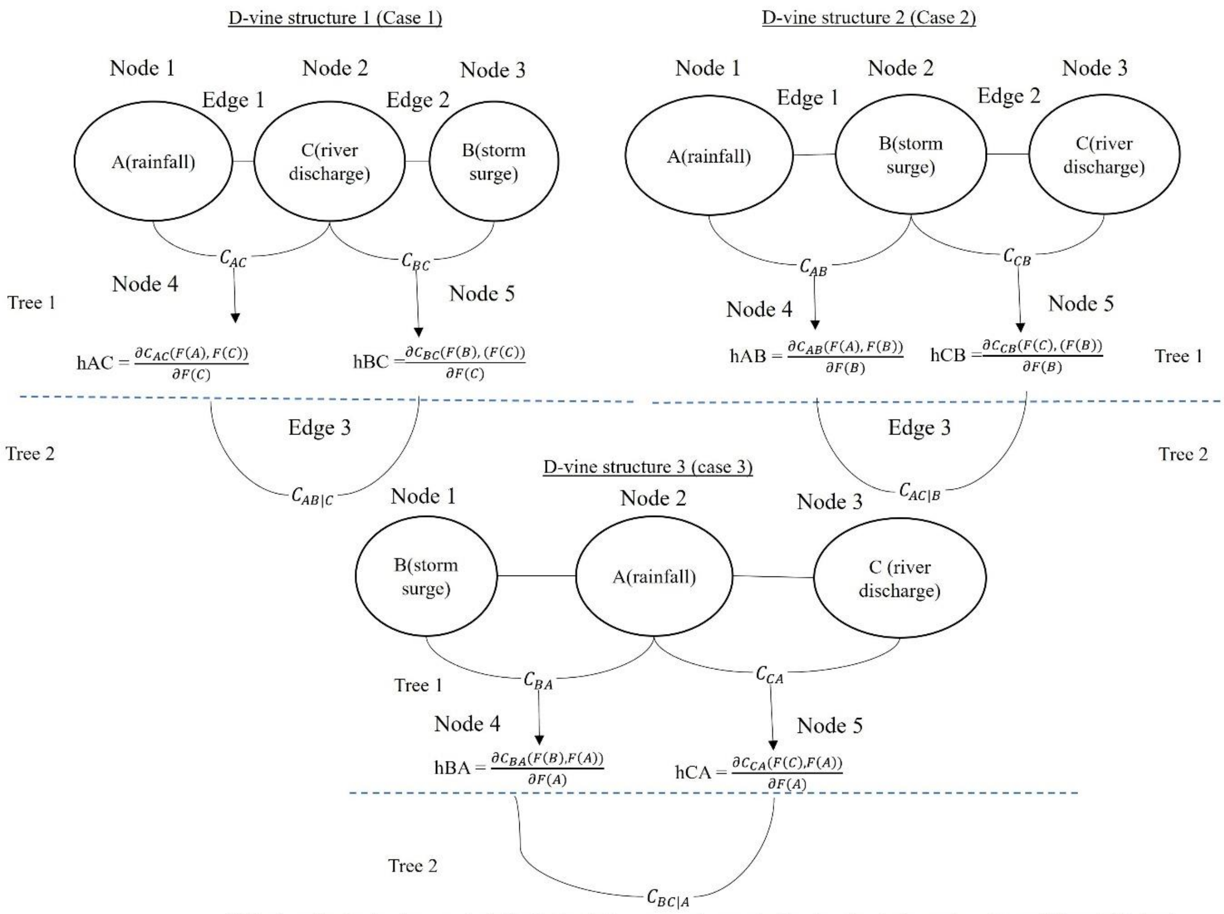

- F(A) = best fitted univariate marginal distribution (using parametric or univariate functions) of annual maximum 24-hr rainfall (mm)
- F(B) = best fitted univariate marginal distribution (using parametric or nonparametric functions) of maximum storm surge (Time interval = ± 4 days)
- F(C) = best fitted univariate marginal distribution (using parametric or nonparametric functions) of maximum river discharge (Time interval = ± 4 days)
- C_{AC} (best fitted 2-D copula between flood pair A and C; C_{BC} (between B and C); C_{AB} (between A and B).
- hAC = conditional cumulative distribution functions (CCDF) estimated using the partial derivatives of C_{AC} w.r.t F(C); hAB = CCDF using partial derivative of C_{AC} w.r.t to F(B); hBC = CCDF using partial derivative of C_{BC} w.r.t to F(C); hBC = CCDF using partial derivative of C_{BC} w.r.t to F(B); hBA = CCDF using partial derivative of C_{BA} w.r.t to F(A); hCA = CCDF using partial derivative of C_{CA} w.r.t to F(A);

Figure 2: Schematic diagram in the 3-D D-vine copula simulation for three different cases [Note: each case of the D-vine structure is defined by permutating the location of the conditional variable, for instance, D-vine structure-1 (River discharge as conditioning variable), D-vine structure -2 (Storm surge as conditioning variable), D-vine structure-3 (Rainfall events as conditioning variable)].

In Equation (11), the conditional cumulative distribution functions f(b|a) and f(c|a, b) are estimated using the pair-copula densities. Also, F(a), F(b) and F(c) are the fitted univariate margins. In Equation (12), C_{ab} is the best-fitted 2-D copula (parametric class or nonparametric) for variables A and B. Our proposed framework selects D-vine with five nodes, three edges, and two tree levels (Refer to Figure 2). The present study constructed a D-vine copula framework for three cases where each case is defined based on permutating the conditioning variables (or variable placed at the centre of the selected D-vine structure, refer to Figure 2). For instance, the D-vine structure 1 (case-1) is defined by selecting and placing the river discharge (RD) as a conditioning variable placed between storm surge (SS) and rainfall (R) events. Similarly, D-vine structure 2 (case 2) and D-vine structure 3 (case 3) are defined by placing storm surge and rainfall events as conditioning variables (refer to Figure 2). This permutation approach to considering each variable of interest as a conditioning variable and selecting the best-fitted vine structure using the fitness test statistics can provide a much more practical and flexible way to the vine copula approach.

Refer to Figure 2 (consider either case) for illustration; the best-fitted univariate flood marginal distribution is selected after selecting the conditioning or centred variable (say B, A, or C). In constructing the D-vine framework nonparametrically, kernel density estimation (KDE), obtained from section 2.2, is selected to define flood marginals. After that, nonparametric copula density (refer to section 2.1) via Bernstein estimator and Beta kernel density estimator is introduced and tested. Thus best-fitted models are selected using the fitness test statistics for different tree levels (Tree 1 and Tree 2, refer to Figure 2).

At first, using the most parsimonious 2-D copulas, either parametric class (refer to Latif and Simonovic [82]) or nonparametric (refer to section 2.1), are selected for each flood pair, say C_{AB} and C_{CB} , the conditional cumulative distribution function (CCDFs), also called the h-function, is estimated [40, 81].

$$F_{A|B}(a,b) = h_{AB} = \frac{\partial C_{A\,B}(F(A),F(B))}{\partial F(B)} \text{ and } F_{C|B}(C,B) = h_{CB} = \frac{\partial C_{C\,B}(F(C),F(B))}{\partial F(B)} \tag{14}$$

In the second Tree 2 level (refer to Figure 2), the CCDFs statistics estimated from Tree 1 level, using copula C_{AB} and C_{CB}, is now input to describe another 2-D copula in the modelling of joint dependence of conditional pair (AC∣B), such as $C_{AC|B}$.

In the nonparametric vine copula approach, the 2-D Bernstein copula estimator (refer to Equation 7) and Beta kernel copula density (refer to Equation 3) are tested individually in both tree levels in the D-vine structures (for all three cases, refer to Figure 2). Our recent study tested the adequacy of different parametric copulas, for instance, mono-parametric Archimedean copulas, mixed or bi-parametric Archimedean copulas and rotated versions (by 180 degrees) of mixed Archimedean copulas etc., for the same flood pairs [82]. The best-fitted 2-D copulas from our previous study are now employed in fitting bivariate flood pairs and estimating CCDFs in the first tree level (Tree 1) of the parametric and semiparametric-based vine framework.

Finally, after selecting the most justifiable copula for each tree level for each D-vine structure (case 1, case 2 and case 3) finally, the full trivariate joint density is calculated by

$$C_{A\,B\,C}(a,b,c) = C_{A\,C|B}(F_{A\backslash B}(a,b), F_{C|B}(c,b)) \cdot C_{A\,B} \cdot C_{C\,B} \tag{15}$$

2.4. Trivariate joint return periods

Frequency analysis provides a mathematical relationship between extreme events quantiles and their non-exceedance probabilities (or recursion interval) by fitting the most justifiable univariate or multivariate probability distribution function [83, 84]. The return period measures the mean or average inter-arrival time between the two design events [85]. The univariate return period's validity is questionable in multidimensional extremes like compound flooding due to the joint action of multiple drivers. In our current study, the developed 3-D joint framework is applied to estimate primary return periods, which are further defined in two cases: OR-joint return period and AND-joint return period [86-89]. Different notation of return periods has their own importance that could depend upon the nature of the undertaken problem. For example, just considering an OR-joint return period or an AND-joint return period would be problematic [30]. A practical risk assessment approach must be demanding to consider a different approach in the return period estimations; readers are advised to follow Graler et al. [40] and Requena et al. [90].

Consider the trivariate events $(A \geq a \text{ OR } B \geq b \text{ OR } C \geq c)$ where either of the events exceeds a specific threshold value; the OR- joint return periods are estimated using the trivariate joint exceedance probability given below

$$T_{A,B,C}^{OR}(a,b,c) = \frac{1}{P\ (A\geq a \vee B\geq b \vee C\geq c)} = \frac{1}{(1-C(F(a),F(b),F(c))} \tag{16}$$

Where $C(F(a), F(b), F(c))$ is the trivariate joint cumulative distribution function (JCDF) estimated using the best-fitted 3-D vine copula structure.

Similarly, consider another trivariate joint dependency case $(A \geq a \text{ AND } B \geq b \text{ AND } C \geq c)$ where all the events exceed a specific threshold value simultaneously; the AND-joint return periods are estimated by considering both trivariate joint cumulative distribution function (JCDF) and bivariate JCDFs which are defined for each random flood pairs given below

$$T_{A,B,C}^{AND}(a,b,c) = \frac{1}{P\ (A\geq a \wedge B\geq b \wedge C\geq c)} = \frac{1}{(1-F(a)-F(b)-F(c)+C(F(a),F(b))+C(F(b),F(c))+C(F(a),F(c))-C(F(a),F(b),F(c))} \tag{17}$$

In Equation (17), $C\big(F(a),F(b)\big), C\big(F(b),F(c)\big)$ *and* $C\big(F(a),F(c)\big)$ is the bivariate (JCDFs) obtained by fitting most parsimonious 2-D copulas to targeted random pairs and $C(F(a), F(b), F(c))$ is the JCDF using the fitted 3-D copula density.

3. Application

3.1. Study area and define compound hazard scenario

The complex interplay between oceanographic, fluvial, and pluvial factors increases the risk of extreme devastation in low-lying coastal communities worldwide. This study introduces a nonparametric approach to constructing a 3-D vine copula framework in compounding the collective impact of rainfall, storm surge and river discharge in flooding events. Our work introduces 46 years of selected flood characteristics collected on west Canada's coast in the trivariate joint probability analysis. The low-lying region near the Pacific coast and Fraser River are highly susceptibilities to flooding and often encounters mature and large-extra tropical storms. Fraser River is the longest river in the south of Metro Vancouver, BC, with an annual discharge at its river mouth of 3550 $m^3 sec^{-1}$. This study searches the dependency for the annual maximum 24-hr rainfall events and their associated river discharge and storm surge events observed within a time lag of ± 4 days from the date of annual maximum 24-hr rainfall events.

Preprints (www.preprints.org) | NOT PEER-REVIEWED | Posted: 12 October 2022 doi:10.20944/preprints202210.0167.v1

At first, the coastal water level (CWL) data is obtained from 1970 to 2018 at the New Westminster tidal gauge station (station id = 7654) with their geographical coordinates (49.2°N Lat and 122.9°W Lon) and delivered by Fisheries and Ocean Canada. Secondly, the storm surge data is estimated by differencing observed CWL data and predicted high astronomical data, which requires proper time matching between them. The Canadian Hydrographic Services (CHS) delivers the predicted tide data, exhibiting two high and two low tides daily. Similarly, the rainfall data is collected at by Haney UBC RF Admin gauge station (49°15′52.1′′N Lat and 122°34′400′′ W Lon). Both storm surge data and rainfall data are collected for the same calendar year. Third, Environment and Climate Change Canada provide the streamflow discharge data collected at the Fraser River at Hope (49°23′09′′N Lat and 121°27′15′′W Lon). It should be noted that the nearest rainfall gauge station and streamflow discharge station are selected within a radial distance of 50 km centring the selected tidal gauge station.

The annual maximum 24-hr rainfall is defined for each year using the daily-basis rainfall amount. The river discharge and storm surge data are now selected by observing their maximum value within a time lag of ±4 days from the date of annual maximum 24-hr rainfall events. Supplementary Table (S.T. 1) lists the descriptive statistics of targeted compound flood (CF) driving agents. Supplementary Figures (SF1, SF2 (a-c) and SF3 (a-c)) illustrate the box plots, histogram plots and normal quantile-quantile (Q-Q) plots. From figure SF3(c) it is found that river discharge observation exhibited more deviation from normality compared to storm surge (SF b) and rainfall events (SF a).

3.2. Nonparametric estimation in the univariate flood marginals

Modelling the univariate flood marginal is a statistical procedure to infer the population based on a finite random sample and is often a mandatory pre-requisite. Our previous study, using the same dataset, confirmed that annual maximum 24-hr rainfall and maximum river discharge events exhibit no serial correlation and zero monotonic trends within its time series [82]. Conversely, maximum storm surge (Time interval = ± 4 days) events have zero serial correlation but exhibit monotonic time trend behaviour, which is estimated using the nonparametric Mann-Kendall (M-K) test [91, 92] at 5% significance level (or 95% confidence interval). Besides this, homogeneity tests for the given time series are examined to identify if changes occur within the time series of flood characteristics, using Pettitt's test [93], SNHT (Standard Normal Homogeneity Test) [94] and Buishand's test [95], refer to Supplementary Table (ST 2). It is found that both rainfall and river discharge events exhibited homogenous behaviour, but storm surge events showed non-homogenous characteristics. In the second row of Table ST 2, the estimated p-value for storm surge events is less than ($p = 0.05$) for both the Pettit and SNHT tests. In conclusion, independent and identical distribution (i.i.d) must be required before introducing it into the probability distribution framework. Thus, a pre-whitening procedure is adopted to remove non-stationarity or de-trend storm surge observation [82].

Table 1 introduces some frequently used kernel density estimations (KDE) whose efficacy is tested in this study to model univariate flood margins. The bandwidth of the fitted KDE is estimated using the direct plug-in (DPI) algorithm; refer to section 2.2. Tables 2 (a-c) list the fitted KDE and their estimated bandwidth. The adequacy of the fitted nonparametric KDE models is tested by comparing empirical and theoretical probabilities. The Gringorten-based position-plotting approach estimates the empirical probabilities for each flood characteristic [94]. The cumulative distribution function (CDF) of the fitted KDE is estimated via

Preprints (www.preprints.org) | NOT PEER-REVIEWED | Posted: 12 October 2022 doi:10.20944/preprints202210.0167.v1

a numerical integration technique or empirical approach because of the lack of a closed form of probability density and cumulative distribution [49]. The goodness-of-fit (GOF) test, such as Mean square error (MSE), root mean square error (RMSE), Akaike information criterion (AIC), Bayesian information criterion (BIC), Hannan-Quinn information criterion (HQC) and Mean absolute error (MAE), are estimated for each fitted model [97-101], refer to Tables 2(a-c). It is found that Normal KDE performed better (minimum value of MSE, RMSE, AIC, BIC, HQC and MAE statistics) and is selected in defining marginal probability density function (PDF) of the maximum 24-hr rainfall, maximum storm surge (Time interval = ± 4 days) and maximum storm surge (Time interval = ± 4 days) events. The qualitative or graphical investigation, using the comparative CDF plots and probability-probability (P-P) plots (refer to Supplementary Figures (SF 4 (a-c) and SF 5 (a-c))), confirms the suitability of the selected Normal KDE.

Table 2: Fitting univariate kernel density estimation (KDE) and their goodness-of-fit (GOF) test for (a) Annual maximum 24-hr Rainfall (mm) (b) Maximum Storm surge (Time interval = ± 4 days) (m) (c) Maximum River discharge (Time interval = ± 4 days) ($m^3 sec^{-1}$)

(a)

Nonparametric KDE	Estimated Bandwidth (via Direct-plug-in method)	MSE (Mean square error)	RMSE (Root mean square error)	AIC (Akaike information criterion)	BIC (Bayesian information criterion)	HQC (Hannan-Quinn information criterion)	MAE (Mean absolute error)
Normal*	**11.25**	**0.0003**	**0.0199**	**-358.22**	**-356.39**	**-357.53**	**0.015**
Epanechnikov (or parabolic)	24.90	0.0007	0.0281	-326.36	-324.53	-325.67	0.023
Biweight (or Quartic)	29.50	0.0010	0.0316	-315.56	-313.73	-314.88	0.026
Triweight	33.50	0.0011	0.0342	-308.42	-306.59	-307.73	0.027
Parametric GEV (Latif and Simonovic 2022B)**	Estimated parameters via Maximum likelihood estimation (MLE)	0.0009	0.0312	-312.97	-307.48	-310.91	0.024

Preprints (www.preprints.org) | NOT PEER-REVIEWED | Posted: 12 October 2022 doi:10.20944/preprints202210.0167.v1

	location (mu $=\mu$) = 1494.64; scale (sigma = σ) = 616.37; shape (xi = ξ) = 0.31						

Note: Normal KDE (bold letter with single asterisk*) outperformed (minimum value of MSE, RMSE, AIC, BIC, HQC and MAE), thus selected in defining the univariate marginal distribution of Annual maximum 24-hr Rainfall (mm) events.

Also, the GEV distribution (double asterisk **) was selected as best-fitted when comparing the performance of different 1-D parametric family distributions in modelling Annual maximum 24-hr Rainfall (mm) events (Latif and Simonovic 2022b).

(b)

Nonparametric KDE	Estimated Bandwidth (via Direct-plug-in method)	MSE (Mean square error)	RMSE (Root mean square error)	AIC (Akaike information criterion)	BIC (Bayesian information criterion)	HQC (Hannan-Quinn information criterion)	MAE (Mean absolute error)
Normal*	**0.07**	**0.0003**	**0.0175**	**-369.83**	**-368.00**	**-369.15**	**0.014**
Epanechnikov (or parabolic)	0.16	0.0007	0.0265	-331.95	-330.12	-331.26	0.020
Biweight (or Quartic)	0.20	0.0008	0.0288	-324.17	-322.34	-323.48	0.022
Triweight	0.22	0.0009	0.0304	-319.30	-317.47	-318.61	0.023
Parametric Normal (Shahid and Simonovic 2022b)**	Estimated parameters via Maximum likelihood estimation (MLE)	0.0011	0.034	-306.56	-302.90	-305.19	0.026

Preprints (www.preprints.org) | NOT PEER-REVIEWED | Posted: 12 October 2022 doi:10.20944/preprints202210.0167.v1

	mean (mu = μ) = 2.340757e-18; sd (sigma = σ) = 1.676386e-01						

Note: Normal KDE (bold letter with single asterisk*) outperformed (minimum value of MSE, RMSE, AIC, BIC, HQC and MAE), thus selected in defining the univariate marginal distribution of Maximum Storm surge (Time interval = ± 4 days)

Also, Normal distribution (double asterisk **) selected as best-fitted when comparing the performance of different 1-D parametric family distributions in modelling storm surge events (Latif and Simonovic 2022b).

(c)

Nonparametric KDE	Estimated Bandwidth (via Direct-plug-in method)	MSE (Mean square error)	RMSE (Root mean square error)	AIC (Akaike information criterion)	BIC (Bayesian information criterion)	HQC (Hannan-Quinn information criterion)	MAE (Mean absolute error)
Normal*	**340.21**	**0.0005**	**0.0223**	**-347.61**	**-345.78**	**-346.93**	**0.017**
Epanechnikov (or parabolic)	753.16	0.0017	0.0415	-290.65	-288.82	-289.96	0.030
Biweight (or Quartic)	892.25	0.0019	0.0444	-284.42	-282.60	-283.74	0.033
Triweight	1013.19	0.0022	0.0477	-277.81	-275.99	-277.13	0.037
Parametric GEV (Shahid and Simonovic 2022b)**	Estimated parameters via Maximum likelihood estimation (MLE)	0.0008	0.0291	-319.15	-313.67	-317.10	0.022
	location (mu =μ) = 1494.64;						

Preprints (www.preprints.org) | NOT PEER-REVIEWED | Posted: 12 October 2022 doi:10.20944/preprints202210.0167.v1

	scale (sigma = σ) = 616.37; shape (xi = ξ) = 0.31						
Note: Normal KDE (bold letter with single asterisk*) outperformed (minimum value of MSE, RMSE, AIC, BIC, HQC and MAE), thus selected in defining the univariate marginal distribution of Maximum River discharge (Time interval = ± 4 days). Also, GEV distribution (double asterisk **) was best fitted when comparing the performance of different 1-D parametric family distributions in modelling river discharge events (Latif and Simonovic 2022b).							

Our previous study selected the Generalized extreme value (GEV), Normal, and GEV distribution fit best for the same dataset tested in the present study [82]. The nonparametric KDE outperformed when comparing the performance of best-fitted functions from the present study and the previous one (refer to Table 2(a-c)).

3.3 Incorporation of nonparametric vine structure in the trivariate flood dependence

Our previous study, Latif and Simonovic [82] already confirmed the existence of positive dependence between flood attribute pairs which are measured both parametrically via the Pearson correlation coefficient and nonparametric via Kendall's tau (τ), and Spearman's rho (ρ) at a 5% significance level (95% confidence interval). At first, the nonparametric via 2-D Bernstein estimator and Beta kernel estimator (refer to Equations 7 and 3) are employed in the bivariate dependence modelling of the rainfall-storm surge, storm surge-river discharge, and rainfall-river discharge pairs (refer to Table 3. The Beta kernel density and Bernstein copula estimator can alleviate the risk of boundary bias problems. The Bernstein copula can facilitate higher consistency and better approximate joint structure than the empirical copula. The fitted Beta kernel density bandwidth is examined using the rule of thumb (ROT) approach by minimizing the AMISE statistics (refer to Equation 4 of section 2.1). Similarly, in fitting the 2-D Bernstein copula estimator, their coefficient is adjusted by the approach discussed by Weiss and Scheffer [57].

Table 3: Fitting the nonparametric 2-D copula density and their goodness of fit (GOF) test to the given flood attribute pair

Flood attribute pairs	Nonparametric 2-D copula density	Estimated Bandwidth (only for Beta kernel copula density)	MSE (Mean Square Error)	RMSE (Root Mean Square Error)	MAE (Mean Absolute Error)	K-S (Kolmogorov–Smirnov)	NSE (Nash–Sutcliffe model efficiency coefficient)

Annual Maximum 24-hr Rainfall (mm)-Maximum Storm surge (Time interval = ± 4 days) (m)	**Bernstein estimator***	0.11	**0.0013**	**0.0360**	**0.0290**	**D = 0.0869, p-value = 0.99**	**0.980**
	Beta kernel density		0.0014	0.0371	0.0295	D = 0.1521, p-value = 0.66	0.979
Maximum Storm surge (Time interval = ± 4 days) (m)-Maximum River discharge (Time interval = ± 4 days) (m3/sec)	**Bernstein estimator***	0.12	**0.0012**	**0.0350**	**0.0270**	**D = 0.1521, p-value = 0.66**	0.981
	Beta kernel density		0.0014	0.0375	0.0295	D = 0.1521, p-value = 0.66	0.978
Annual Maximum 24-hr Rainfall (mm)-Maximum River discharge (Time interval = ± 4 days) (m3/sec)	Bernstein estimator	0.17	0.0011	0.0338	0.0258	D = 0.1956, p-value = 0.34	0.981
	Beta kernel density*		**0.0008**	**0.0298**	**0.0221**	**D = 0.1521, p-value = 0.66**	**0.985**
Note: Bernstein copula estimator (bold letter with an asterisk) fitted best for flood pairs rainfall and storm surge, and storm surge and river discharge. Beta kernel copula density is most parsimonious for flood pair rainfall and river discharge.							

Both nonparametric models' performance is evaluated using different GOF measures, for instance, MSE, RMSE, MAE, KS (Kolmogorov–Smirnov) [102] and NSE (Nash–Sutcliffe model efficiency coefficient) [103], refer to Table 3. The Bernstein copula estimator's performance is better for flood pairs (rainfall and storm surge) and (storm surge and river discharge) (minimum value of MSE, RMSE, MAE and KS test value and high NSE test statistics). However, according to Table 3, the performance of the Beta kernel density outperformed Bernstein estimator for flood pair rainfall and river discharge.

We constructed the D-vine copula for three cases, where each case defines a D-vine structure by permutating the location of conditioning variables. All the computation involved in the establishment of 3-

Preprints (www.preprints.org) | NOT PEER-REVIEWED | Posted: 12 October 2022 doi:10.20944/preprints202210.0167.v1

D vine copula (also in fitting 2-D nonparametric copula density) is carried out using the R software [104] with library "kdecopula" [105] and "kdevine" [106].

1. D-Vine structure 1 (Case-1) considers river discharge event as a conditioning variable by placing it at the centre of the vine structure (refer to Figure 2 and Tables 3 and 4). In this structure, at first, the 2-D Beta kernel copula density and 2-D Bernstein copula estimator, which are selected as best-fitted from Table 3 for flood pair rainfall-river discharge and storm surge-river discharge in the first tree level (Tree 1), are now employed in the estimation of conditional cumulative distribution functions (CCDFs), $h_{\text{RAIN RIVER DISCHARGE}}$ and $h_{\text{STORM SURGE RIVER DISCHARGE}}$ (refer to Equation 14). The copula in the second tree level (Tree 2) is now identified using the above estimated CCDDFs values as input. It is found that the Bernstein copula estimator outperformed Beta kernel density to model joint dependence for the flood pair (RAIN, STORM SURGE|RIVER DISCHARGE), $C_{\text{RAIN STORM SURGE|RIVER DISCHARGE}}$ (which exhibited the minimum value of MSE, RMSE, MAE, and KS and the higher value of NSE test statistics). Finally, the full 3-D trivariate joint density is obtained using Equation 15.
2. Similarly, D-vine structure 2 (Case-2) comprises storm surge event as a conditioning variable (refer to Tables 3 and 4 and Figure 2). In this vine framework, at first, in the first tree level (Tree 1), the Bernstein estimator is identified as the most justifiable and thus is employed in the estimation of CCDFs $h_{\text{RAIN, STORM SURGE}}$ and $h_{\text{RIVER DISCHARGE, STORM SURGE}}$, followed by Equation 14. Secondly, in the second tree level (Tree 2), the Bernstein copula estimator is selected as the most parsimonious in establishing the dependence between of flood pair (RAIN RIVER DSICHARGE|STORM SURGE), $C_{RAIN\ RIVER\ DSICHARGE|STORM\ SURGE}$. Finally, using Equation 15, the full trivariate joint density of the fitted vine structure is estimated.
3. D-Vine structure 3 (case 3) is defined by considering rainfall event as a conditioning variable placed in the centre of the selected D-vine structure (refer to Figure 2, and Tables 3 and 4). Bernstein estimator and Beta kernel density are identified as most justifiable and thus employed in the estimation CCDFs, $h_{\text{STORM SURGE, RAINFALL}}$ and $h_{\text{RIVER DISCHARGE, RAIN}}$ (followed by Equation 14) in Tree 1. In the second level (Tree 2), again Bernstein copula estimator is identified as the most parsimonious in modelling joint dependence of flood pair (STORM SURGE RIVER DSICHARGE|RAINFALL) (refer to Table 4). Finally, followed by Equation (15), the full trivariate joint density of the fitted vine structure is defined.

Table 4: Summary statistics in the nonparametric D-vine structure for three different cases by incorporating the Bernstein estimator and Beta kernel density (each D-vine structure is defined by permutating the location of the conditioning variable)

	Vine Structure (Conditioning variable)	Tree Level	Flood attribute pairs	Fitted nonparametric copula estimator	Estimated Bandwidth (for Beta kernel copula density)	MSE (Mean Square Error)	RMSE (Root Mean Square Error)	MAE (Mean Absolute Error)	K-S (Kolmogorov–Smirnov)	NSE (Nash–Sutcliffe model efficiency coefficient)

Preprints (www.preprints.org) | NOT PEER-REVIEWED | Posted: 12 October 2022 doi:10.20944/preprints202210.0167.v1

Case 1 (1-3-2)	3 or Maximum River Discharge (Time interval = ± 4 *Days*) placed in the centre	Tree 1	1-3 (Rain-River discharge)	Beta kernel	0.11	0.0004	0.0223	0.017	D = 0.086, p-value = 0.99	0.992
			2-3 (storm surge-river discharge)	Bernstein		0.0006	0.0249	0.019	D = 0.087, p-value = 0.99	0.990
		Tree 2	$12 \mid 3$	Bernstein						
				Beta kernel						
Case 2 (1-2-3)*	2 or Maximum Storm Surge (Time interval = ± 4 *days*) placed in the centre	Tree 1	1-2 (Rain – Storm Surge)	Bernstein	0.17	**0.0002**	**0.0153**	**0.013**	**D = 0.152, p-value = 0.66**	**0.995**
			3-2 (Storm surge – river discharge)	Bernstein		0.0003	0.0154	0.013	D = 0.152, p-value = 0.66	0.995
		Tree 2	$13 \mid 2$	**Bernstein**						
				Beta kernel						
Case 3 (2-1-3)	1 or Annual Maximum 24-hr Rainfall placed in the centre	Tree 1	2-1 (Storm surge-Rain)	Bernstein	0.12	0.0004	0.0203	0.015	D = 0.152, p-value = 0.66	0.993
			3-1 (River discharge-Rainfall)	Beta kernel		0.0005	0.0214	0.016	D = 0.086, p-value = 0.99	0.992
		Tree 2	$23 \mid 1$	Bernstein						
				Beta kernel						

Note: D-vine structure-2 (case-2) (bold letter with an asterisk) selected the most parsimonious vine density (exhibits the minimum value of MSE, RMSE MAE, K-S and high value of NSE test statistics)

After approximating three different D-vine structures (case 1, case 2 and case 3), their performance is compared using the fitness test statistics (MSE, RMSE, MAE, NSE and K-S). The theoretical probability (CDF) is estimated using a developed 3-D vine structure for each case and compared with empirical observations in estimating the GOF test statistics. Table 4 shows that the D-vine structure for case-2, considering storm surge as a conditioning variable, performed better than other D-vine structures. The selected structure exhibited a minimum MSE, RMSE, and MAE value and a high NSE test value. The above approach in the vine copula provides much better flexibility in selecting the best vine model, not just by fixing the conditioning variable but by switching or permutating the conditioning variable. For example, in the above case, when considering storm surges as conditioning variables, the performance of the fitted D-vine copula gets better than considering either rainfall or river discharge events. Supplementary Figure (SF 8) illustrate the vine tree plot of the developed D-vine structure in the nonparametric fitting procedure.

3.4. *Comparing the adequacy of fitted Nonparametric D-vine with parametric and semiparametric approaches in the D-vine copula framework*

3.4.1. Constructing a D-vine structure in the parametric fitting procedure

In the parametric vine approach, at first, the best-fitted univariate marginal pdfs, for instance, GEV (for rainfall event), Normal (for storm surge event), and GEV (for river discharge event) distribution, are selected (refer to Tables 2(a-c)). Followed by the same steps we discussed in the last section, 3.3, three different D-vine structures (case 1, case 2 and case 3) are considered by permutating the conditioning variables (refer to Figure 2). Our previous study confirms that Survival BB7 fit best for flood pair rain and river discharge, Survival BB1 for storm surge-river discharge, and BB1 copula for rain and storm surge pair [82].

Table 5: Summary statistics of the fitted D-vine structure under parametric distribution settings (via parametric copulas with parametric marginal distributions)

	Vine Structure (Conditioning variable)	Tree Level	Flood attribute pairs	Most parsimonious fitted copula	Copula dependence parameters (θ) via MPL	MSE	RMSE	MAE	K-S	NSE	*Log-likelihood (LL)*	*AIC*	*BIC*
Case 1 (1-3-2)	3 or Maximum River Discharge (Time interval = $\pm 4\ Days$) placed in the centre	Tree 1	1-3 (Rain-River discharge)	Survival BB7	$\theta(theta) = par = 1.142$; $\delta(delta) =$ par2 = 0.19	0.00086	0.0294	0.021	D = 0.152 (0.66)	0.982	10.51	-11.02	-1.87
			3-2 (storm surge-river discharge)	Survival BB1	$\boldsymbol{\theta(theta)}$= par= **0.23**; $\boldsymbol{\delta(delta)}$= par2 = **1.29**								
		Tree 2	12|3	Frank	$\theta(theta) = par =$ **2.92**								
Case 2	2 or Maximum Storm	Tree 1	1-2 (Rain – Storm Surge)	BB1 (Clayton-Gumbel)	$\theta = theta = 0.19$	0.00088	0.0297	0.022	D = 0.173 (0.48)	0.982	10.50	-11.01	-1.

(1-2-3)	Surge (Time interval = $\pm 4\ days$) placed in the centre				; $\delta = delta =$ 1.36								87
			2-3 (Storm surge – river discharge)	Survival BB1	$\boldsymbol{\theta(theta)}$= par= $\mathbf{0.23}$; $\boldsymbol{\delta(delta)}$= par2 = **1.29**								
		Tree 2	13|2	Rotated BB6 270 degrees	$\boldsymbol{\theta(theta)}$= par= -1; $\boldsymbol{\delta(delta)}$= par2 = -1								
Case 3 (2-1-3)*	1 or Annual Maximum 24-hr Rainfall placed in the centre	Tree 1	2-1 (Storm surge-Rain)	BB1 (Clayton-Gumbel)	$\theta(par) = theta = 0.19$; $\delta(par2) = delta = 1.36$	**0.00084**	**0.0290**	**0.021**	**D = 0.152 (0.67)**	**0.982**	**10.85**	**-11.71**	**-2.57**
			3-1 (River discharge-Rainfall)	Survival BB7	$\theta(theta) = par = 1.142$; $\delta(delta) = par2 = 0.19$								
		Tree 2	23|1(Storm-River/Rainfall)	Frank	$\theta(par) = theta = 2.97$								

Note: D-vine structure-3 (case 3), considering rainfall events as a conditioning variable, perform better (minimum value of AIC, BIC, HQC, MSE, RMSE, K-S and high value of model's L-L and NSE statistics)

For vine structure 1 (case 1, river discharge as conditioning variable, refer to Figure 2 and Table 5), both the selected 2-D copulas (Survival BB7 and Survival BB1) are employed in the estimation CCDFs, which become input to define another 2-D copula in the second tree level (Tree 1). The present study tests different parametric copulas to fit the D-vine structure's second tree level (Tree 2) (refer to Supplementary Tables ST 3(a-c)). The parameters of the fitted copulas are estimated using maximum pseudo-likelihood estimation (MPL) [107, 108], and the performance of the fitted models is compared using the Cramer-von Mises (CvM) functional test statistics S_n, with the parametric bootstrap procedure (N is the number of bootstrap samples = 1000) [109-110]. From Tables ST 3(a-c), the Frank copula is identified as best for Tree 2 (D-vine structure 1, case 1), rotated BB6 270 degrees copula for Tree 2 (D-vine structure 2, case 2), and Frank copula is best fitted (D-vine structure 3, case 3). The full trivariate D-vine structure (parametric settings) for each case is obtained using Equation 15.

After developing vine structures for the given flood characteristics, their performance is compared to select the most efficient D-vine structure developed under parametric settings for three cases. From Table 5, it is found that D-vine structure-3 (case-3), rainfall as a conditioning variable, outperformed other parametric vine structures (minimum value of AIC, BIC, MSE, RMSE, MAE, K-S statistics and with a high value of log-likelihood (L-L) and NSE statistics).

Preprints (www.preprints.org) | NOT PEER-REVIEWED | Posted: 12 October 2022 doi:10.20944/preprints202210.0167.v1

3.4.2. Constructing D-vine structure in the semiparametric settings

2-D parametric class copulas are incorporated with nonparametric marginals pdf in the semiparametric D-vine structure. Firstly, the best-fitted 2-D parametric copulas for Tree-1 in all three cases of D-vine structure (refer to Figure 2), are selected from our previous study [82], also refer to section 3.4.1. Supplementary Table (ST 4(a-c))) fitted different parametric class 2-D copula with MPL-based parameter estimation procedure in estimating the most justifiable bivariate density fitted to the second tree level (Tree 2). The investigation found that the Frank copula is selected best for D-vine structure-1 (case-1), rotated BB6 270 degrees for vine structure-2 (case-2) and the Frank copula for D-vine structure-3 (case-3). Using Equation 15, the full trivariate vine copula joint density is estimated for each fitted D-vine structure. The most justifiable semiparametric-based vine structure is selected by comparing the performance of three different cases of D-vine structure. Table 6 provides the summary details of the fitted D-vine structures. It is found that D-vine structure 3 (case-3), considering rainfall as a conditioning variable, outperforms all other possible D-vine structures (case-1 and case-2); it exhibited a minimum value of MSE, RMSE, MAE., K-S, AIC. and BIC statistics and a high value of model likelihood (L-L) and NSE statistics.

Table 6: Details of the fitted 3-D vine structure in the semiparametric distribution settings for three different cases

	Vine Structure (Conditioning variable)	*Tree Level*	*Flood attribute pairs*	*Most parsimonious or Best-fitted copula*	*Copula dependence parameters* (θ)	*MSE*	*RMSE*	*MAE*	*K-S*	*NSE*	Log-likelihood (LL)	AIC (Akaike information criterion)	BIC (Bayesian information criterion)
Case 1 (1-3-2)	3 or Maximum River Discharge (Time interval = $\pm 4\ Days$) placed in the centre	Tree 1	1-3 (Rain-River discharge)	Survival BB7	$\theta(theta) = par =$ 1.142; $\delta(delta) =$ par2 = 0.19	0.0006	0.0236	0.0185	D = 0.152 (0.66)	0.9886	10.68	-11.37	-2.23
			3-2 (storm surge-river discharge)	*Survival BB1*	$\boldsymbol{\theta(theta)}$= par= **0.23**; $\boldsymbol{\delta(delta)}$= par2 = **1.29**								
		Tree 2	12|3	Frank	$\theta(theta) = par =$ **2.89**								

Preprints (www.preprints.org) | NOT PEER-REVIEWED | Posted: 12 October 2022 doi:10.20944/preprints202210.0167.v1

Case 2 (1-2-3)	2 or Maximum Storm Surge (Time interval = $\pm 4\ days$) placed in the center	Tree 1	1-2 (Rain – Storm Surge)	BB1 (Clayton - Gumbel)	$\theta =$ $theta =$ 0.19; $\delta =$ $delta =$ 1.36	0.0006	0.0239	0.0192	D = 0.130 (0.82)	0.9883	10.81	-9.62	1.34
			2-3 (Storm surge – river discharge)	*Survival BB1*	$\boldsymbol{\theta}(\boldsymbol{theta})$= par= **0.23**; $\boldsymbol{\delta}(\boldsymbol{delta})$= par2 = **1.29**								
		Tree 2	13|2	Rotated BB6 270 degrees	$\boldsymbol{\theta}(\boldsymbol{theta})$= par= -1; $\boldsymbol{\delta}(\boldsymbol{delta})$= par2 = -1								
Case 3 (2-1-3)*	1 or Annual Maximum 24-hr Rainfall placed in the center	Tree 1	2-1 (Storm surge-Rain)	BB1 (Clayton - Gumbel)	$\theta(par) =$ $theta =$ 0.19; $\delta(par2) =$ $delta =$ 1.360	**0.0005**	**0.0232**	**0.0185**	**D = 0.1303 (0.82)**	**0.9890**	**11.38**	**-12.77**	**-3.62**
			3-1 (River discharge-Rainfall)	Survival BB7	$\theta(theta) =$ $par =$ 1.14; $\delta(delta) =$ par2 = 0.19								
		Tree 2	23|1	Frank	$\theta(par) =$ $theta =$ 2.75								

Note: D-vine structure 3 (case 3) fitted best (bold letter with an asterisk) (minimum value of AIC, BIC, MSE, RMSE, MAE, K-S and high value of NSE and L-L statistics.

3.4.3. *Comparison of model's performance (nonparametric vs semiparametric vs parametric vine)*

Previous sections 3.3, 3.4.1, and 3.4.2 recognized the most justifiable vine structure, D-vine structure-2 (obtained via nonparametric vine approach), D-vine structure-3 (via parametric vine approach) and D-vine structure-3 (via semiparametric framework). This section performed an analytical and graphical comparison to check the adequacy of the selected nonparametric D-vine density with parametric and semiparametric vine approaches fitted to the given triplet flood variables. Refer to Table 7; it is observed that the D-vine structure (case-2) defined in the nonparametric setting outperformed (minimum value of MSE, RMSE, K-S, MAE and high NSE test statistics). It is also observed that the performance of the selected semiparametric D-vine structure (case-2) is better than the parametric D-vine structure (case-2) in the trivariate flood dependence. These results can further reveal how well the incorporated vine's performance improves, when switching its marginal distribution from parametric to nonparametric, and copula joint density from parametric to nonparametric joint pdf.

The reliability and suitability of the selected D-vine structures are examined further by comparing Kendall's τ correlation coefficient estimated from the simulated flood events (sample size N = 1000) using the best-fitted nonparametric vine copula (D-vine structure-2), parametric vine (D-vine structure-2) and semiparametric vine copula (D-vine structure-3) and compared with the empirical Kendall's τ coefficient estimated from the historical flood events (refer to Table 8). It is found that the obtained nonparametric D-vine structure (case-2) exhibits a minimum gap or difference between the empirical and theoretical Kendall's tau statistics. These results confirm that the selected nonparametric vine structure regenerates the historical flood dependence structure (or correlation) much more efficiently. The same table also revealed that the semiparametric vine approach better captures and regenerates flood dependence than parametric vine copula density.

Table 7: Comparing the performance of the selected nonparametric D-vine structure with parametric and semiparametric vine copula density

Best-fitted D-vine structure	MSE	RMSE	MAE	K-S	NSE
Nonparametric settings (D-vine structure-2 (case-2)*	**0.0002**	**0.0153**	**0.0130**	**D = 0.152, p-value = 0.66**	**0.995**
Semiparametric settings (D-vine structure-3 (case-3)	0.0005	0.0232	0.0185	D = 0.130 (0.82)	0.989
Parametric settings (D-vine structure-3 (case-3)	0.00084	0.0290	0.0218	D = 0.152 (0.67)	0.982
Note: D-vine structure-2 derived in the nonparametric settings outperformed both parametric and semiparametric approaches in the D-vine structure for trivariate CF events					

Table 8: Examining the reliability of the developed D-vine structure (nonparametric settings) vs parametric D-vine vs semiparametric D-vine copula framework by comparing Kendall's τ correlation coefficient estimated using the generated random samples (size N= 1,000) obtained from the above-selected model with Empirical Kendall's τ values estimated from historical observations

CF pairs	Kendall's tau estimated from historical flood events (Empirical estimates)	Kendall's tau estimated from best-fitted D-vine copula (D-vine structure 3)	Kendall's tau calculated from best-fitted D-vine copula (D-vine structure-3) in a semiparametric	Kendall's tau estimated from best-fitted D-vine copula (D-vine structure-2) in the nonparametric

		in a parametric setting (Theoretical estimates)	setting (Theoretical estimates)	setting (Theoretical estimates)
Annual maximum 24-hr rainfall (mm)c-Maximum Storm Surge (m) (Time interval = $\pm 4\ days$)	0.30	0.29	0.31	29
Maximum Storm Surge (m) (Time interval = $\pm 4\ days$) $-$ Maximum River discharge (m3/sec) (Time interval = $\pm$ 4 $days$)	0.29	0.34	0.31	29
Annual maximum 24-hr rainfall (mm)c-Maximum Storm Surge (m) (Time interval = $\pm 4\ days$) - Maximum River discharge (m3/sec) (Time interval = $\pm 4\ days$)	0.14	0.16	0.15	0.14
Note: It is clearly found that the best-fitted D-vine structure-2 constructed in the nonparametric distribution setting are very much closer to its empirical estimates.				

Besides this, a graphical visual inspection is carried out to crosscheck the adequacy of the selected D-vine structure-2 obtained nonparametrically. The overlapped scatterplots between the observed samples (via historical flood) and simulated samples (using D-vine structure-2, case-2) of sample size (N = 1000) are obtained; refer to Supplementary Figures (S.F. 6a-c). It is found that D-vine structure-2 (under nonparametric settings) performs adequately since the simulated random sample (indicated by light grey colour) overlapped with the natural mutual concurrency of the historical flood samples (red colour); refer to Figures (S.F. 6 a-c). Supplementary Figure (S.F. 7) illustrate a 3-D scatterplot matrix of the generated flood events (sample size N = 1000) using the selected nonparametric vine model. Supplementary Figure (S.F. 8) illustrate the vine tree structure of the most justifiable D-vine structure in the nonparametric setting.

In conclusion, the above investigations confirm that the nonparametric vine copula density is much better in trivariate dependence analysis of CF events. This framework has no prior distributional assumption about their copula joint density and its marginal behaviour. Finally, the selected nonparametric vine density is employed to estimate trivariate joint cumulative distribution functions (JCDF) and joint return periods. Further, the derived model is used in estimating the failure probability (FP) statistics for assessing the hydrologic risk associated with compound events.

3.5. Compound flooding events risk assessments

Flood frequency analysis (FFA) is the mathematical establishment of an interrelationship between the flood design quantiles and their non-exceedance probabilities or return periods by fitting the best-fitted multivariate probability distribution function. The primary return periods comprise two different joint cases, OR and AND-joint. The best-fitted nonparametric D-vine structure is employed in estimating trivariate joint cumulative distribution function (JCDF) and trivariate return periods for OR- and AND-joint cases for a different possible combination of flood events, refer to Table 9 and Equations 16 and 17.

Preprints (www.preprints.org) | NOT PEER-REVIEWED | Posted: 12 October 2022 doi:10.20944/preprints202210.0167.v1

Table 9 also estimates the bivariate joint return periods using the best-fitted 2-D nonparametric copula density (refer to Table 3). It is found that the trivariate return periods for the AND-joint case are higher than for the OR-joint case for the same flood combination. Similarly, the bivariate AND-joint case is higher than OR-joint for the same flood pair combinations. These results further reveal that the occurrence of trivariate flood events simultaneously is less frequent in the "AND" case and more frequent in the "OR" joint case. The same observations are also valid for the bivariate case. For instance, refer to Table 9, 100-years flood event with following characteristics, rainfall = 147.541 mm, storm surge = 0.337486 m and river discharge = 5951.523 $m^3 sec^{-1}$, the trivariate OR- and AND- joint return period is 33.66 years and 3486.75 years. For the same flood characteristics mentioned above, the bivariate return periods for OR- and AND-joint cases are (50.92 years and 2744.23) for flood pair rainfall and storm surge events, (50.26 years and 9633.91 years) for storm surge and river discharge, and (50.29 years and 8517.88 years) for rainfall and river discharge pair events.

The above results reveal that the accountability of both primary joint return periods is essential; just considering either AND-joint or OR-joint case would be problematic in the hydrologic risk evaluation. They also depend on the nature of water-related problems, which usually decide the importance of the different types of return periods.

Table 9: Comparing primary return periods (univariate vs bivariate vs trivariate) for a different possible combination of triplet flood events.

	Estimated flood quantiles using the inverse cumulative distribution functions (CDFs) of best-fitted marginal distribution via KDE			Bivariate joint return periods (JRPs)						Trivariate joint return periods (JRPs) estimated using the best-fitted D-vine structure (case-2)	
Return period (years), T	Annual Maximum 24-hr Rainfall (R) (mm)	Maximum Storm surge (m) (SS) (Time interval = ±4 days)	Maximum River discharge (RD) ($m^3 sec^{-1}$)(Time interval = ±4 days))	OR-JRP, T_{RS}^{OR}	AND-JRP T_{RS}^{AND}	OR-JRP, T_{SRD}^{OR}	AND-JRP T_{SRD}^{AND}	OR-JRP, T_{RRD}^{OR}	AND-JRP, T_{RRD}^{AND}	OR-JRP, T_{RSRD}^{OR}	AND-JRP, T_{RSRD}^{AND}
5	97.04	0.151	2573.15	3.08	13.17	2.84	20.52	2.88	18.91	2.06	15.95
10	110.73	0.228	3367.54	5.69	40.97	5.32	81.46	5.34	77.23	3.70	50.42
20	128.04	0.277	5408.36	10.77	139.73	10.31	328.39	10.32	318.89	7.02	173.06
50	143.42	0.316	5854.64	25.85	760.16	25.29	2162.62	25.30	2063.98	17.00	950.29
100	147.54	0.337	5951.52	50.92	2744.23	50.26	9633.91	50.29	8517.88	33.66	3486.75

In the hydrologic risk assessments of compound events, consideration of only traditional joint primary return periods would be ineffective in describing the risk of potential flood events during the entire project design lifetime [9, 111]. In recent studies, a hydrologic risk tool called failure probability (FP) statistics [112, 113] is highlighted and used efficiently. FP usually defines the chance of potential flood hazards occurring at least once in a given project design lifetime. FP statistics can define the risk of CF events more appropriately than just visualizing their joint return periods. In our current study, the developed nonparametric D-vine model is employed further in estimating the FP statistics. Few pieces of literature incorporated FP statistics in the bivariate hydrologic risk assessments [9, 114]. Our present study examined variation in the trivariate, bivariate and univariate flood hazard events measured by service design lifetime for different return periods, such as 100 years, 50 years, 20 years, 10 years and 5 years, refer to Figures 3 (a-e). It is found that a trivariate flood hazard scenario results in high-value FP than bivariate and univariate events. Both the trivariate and bivariate (also univariate) hydrologic risk or FP statistics are reduced when the return increases. Also, the FP statistics increase when there is an increase in the service design lifetime of the hydraulic infrastructure under consideration. For instance, at the return period of 100 years, the estimated value of FP statistics is 0.778 (for trivariate hazard scenario) and 0.629 (for bivariate hazard scenario) at a 50-years design lifetime. When considering a higher design lifetime, say 100 years, for the same return periods (100 years), the estimated value is 0.951 (for the trivariate hazard scenario) and 0.862 (for the bivariate scenario). Similarly, at 100-year return periods, the trivariate and bivariate hazard scenario is 0.933 and 0.832 (at 90 years design lifetime). When reducing the return periods to 50 years, the value is 0.995 and 0.971 at the same design lifetime (90 years).

From the above results, it is inferred that ignoring the trivariate joint dependency analysis by integrating the impact of rainfall, storm surge and river discharge would be a problem which could result in the underestimation of FP. Their joint probability occurrence facilitates a better understanding and realization of extreme compound scenarios. All the above-discussed analytical and graphical investigations are crucial for sustainable design and planning in coastal flood management strategies. The derived nonparametric extreme framework can be applied to any coastal region worldwide. Also, the proposed method can be extended to more than three flood-contributing variables that can comprehensively describe the risk of compound events.

4. Research summary and conclusion

This study incorporated D-vine copula in the nonparametric fitting procedure to model trivariate joint probability analysis of the storm surge, river discharge and rainfall in the compound flood risk assessments. A comprehensive compound flood risk understanding can demand the accountability of all the above-mentioned flood-driving agents simultaneously because the complex interplay between them can be devastating. The performance of the parametric and semiparametric approach in the vine framework is also compared with the proposed nonparametric vine density in the CF dependence. The traditional vine framework is defined by incorporating multiple parametric class 2-D copula densities with parametric 1-D univariate margins. Such parametric density (and their marginal distribution) approximation has some statistical constraints already discussed in section 1. The nonparametric via the Bernstein estimator and Beta kernel copula estimator is a much more comprehensive way in the vine construction, where the fitted 2-D copula densities between each flood pair can adapt to any dependence structure without the requirement of any specific or fixed probability density structure. Conversely, the semiparametric vine framework integrates multiple 2-D parametric class copula with nonparametric marginal pdfs via the Kernel density estimation (KDE). The main finds of this study are summarized below:

1. This study developed a trivariate joint probability framework to search the dependency between annual maximum 24-hr rainfall and their associated storm surge and river discharge observed within a time lag of ± 4 days from the date of the highest annual rainfall events. Our previous study examined the degree of mutual concurrencies and confirmed a significant positive correlation between these flood pairs [82].
2. Similarly, our previous study [82] confirmed that rainfall and storm surge events did not exhibit any significant trend and serial correlation. From our present study, it is also confirmed that both variables are homogenous. However, the storm surge events exhibited nonstationary behaviour (time trend with non-homogeneity), but no serial correlation was identified.
3. The nonparametric Normal KDE is most parsimonious for all three flood variables (refer to Table 2a-c). Also, the results are the same when comparing the performance with the best-fitted parametric function (GEV, NORMAL, GEV [82], refer to Tables 2a-c).
4. In this study, the vine copula is constructed by permutating the conditioning variable's location, which results in three different D-vine structures (refer to Table 2). In constructing the D-vine copula nonparametrically (Table 3), it is found that the Bernstein copula fit best for flood pairs (rainfall-storm surge) and (storm surge and river discharge), and the Beta kernel estimator fit best for pair (rainfall-river discharge). All the selected nonparametric 2-D copulas are employed in the 3-D vine construction for three different D-vine structures. Analytical-based G.O.F. test (viz, MSE, RMSE, MAE, K-S and NSE) confirms that nonparametric D-vine structure-2 (case-2) is found to perform better-considering storm surge as a conditioning variable (refer to Table 4) (where Bernstein copula estimator fitted both in the first and second tree level).
5. Similarly, the parametric and semiparametric vine fitting approach select D-vine structure-3 (rainfall as a conditioning variable, refer to Tables 5 and 6) as the most justifiable density based on different GOF test statistics (MSE., RMSE, MAE., K-S, NSE, AIC., BIC., HQC and Model L-L).
6. Best-fitted performances such as nonparametric, semiparametric, and parametric fitting-based D-vine structures are compared analytically using GOF tests (refer to Table 7). Results confirmed the adequacy of the proposed nonparametric vine density. The model's reliability is further investigated analytically by comparing the theoretical, obtained by best-fitted D-vine structures, and empirical Kendall's tau, using the historical observations. Results reveal that the selected D-vine structure-2, in the nonparametric fitting procedure, outperformed (refer to Table 8). In other words, the selected vine structure regenerates historical flood events efficiently. The adequacy of D-vine structure-2 (Nonparametric framework) is further investigated graphically through overlapped scatterplots between historical observation and generated samples (refer to Figure (SF 6)). It is clearly observed that the fitted model effectively captures the natural mutual dependencies of historical flood events. In conclusion, our proposed vine copula density in the nonparametric fitting is a much better alternative to the traditional parametric vine approach.
7. Finally, the best-fitted nonparametric vine density is employed to estimate trivariate primary joint return periods for OR- and AND-joint cases. OR-joint case results in lower return periods than the AND-joint case for the same flood combinations (refer to Tale 9). It is observed how important it is to take accountability for trivariate return periods rather than just considering a bivariate (or univariate) approach, which would be problematic and less efficient in solving different water-related decision-making.
8. The trivariate and bivariate joint CDFs are employed in estimating failure probability (FP) statistics because the traditional definition of primary joint return periods would not explain the risk of

Preprints (www.preprints.org) | NOT PEER-REVIEWED | Posted: 12 October 2022 doi:10.20944/preprints202210.0167.v1

potentially flood hazard scenarios occurring at least once in a given project design lifetime of the infrastructure under consideration. The FP statistics highlight the hydrologic risk due to the compound effect of rainfall storm surge and river discharge events in the trivariate flood events. Investigation reveals that FP statistics could be underestimated if neglecting the trivariate joint probability analysis between targeted flood characteristics compared to when considering the same flood variables in pairwise joint modelling. For instance, the FP statistics are higher when considering trivariate joint distribution for the OR-joint event than when considering bivariate joint dependency between flood pairs. Also, the hydrologic risk (trivariate, bivariate and univariate events) decreases with an increase in the return periods (refer to Figure 3 a-e). At the same time, hydrologic risk increases, followed by the service design lifetime of hydraulic infrastructure under consideration. The same investigation also found that the FP of univariate flood events is much lower than trivariate (and bivariate) events. This further reveals that compound events may not be devastating if each flood source variable is considered separately. Combining more relevant flood-contributing variables and switching from bivariate to trivariate provides a more comprehensive understanding of flood risk. In conclusion, all the above-estimated risk statistics and discussions are essential for coastal flood management planning and sustainable design.

Preprints (www.preprints.org) | NOT PEER-REVIEWED | Posted: 12 October 2022 doi:10.20944/preprints202210.0167.v1

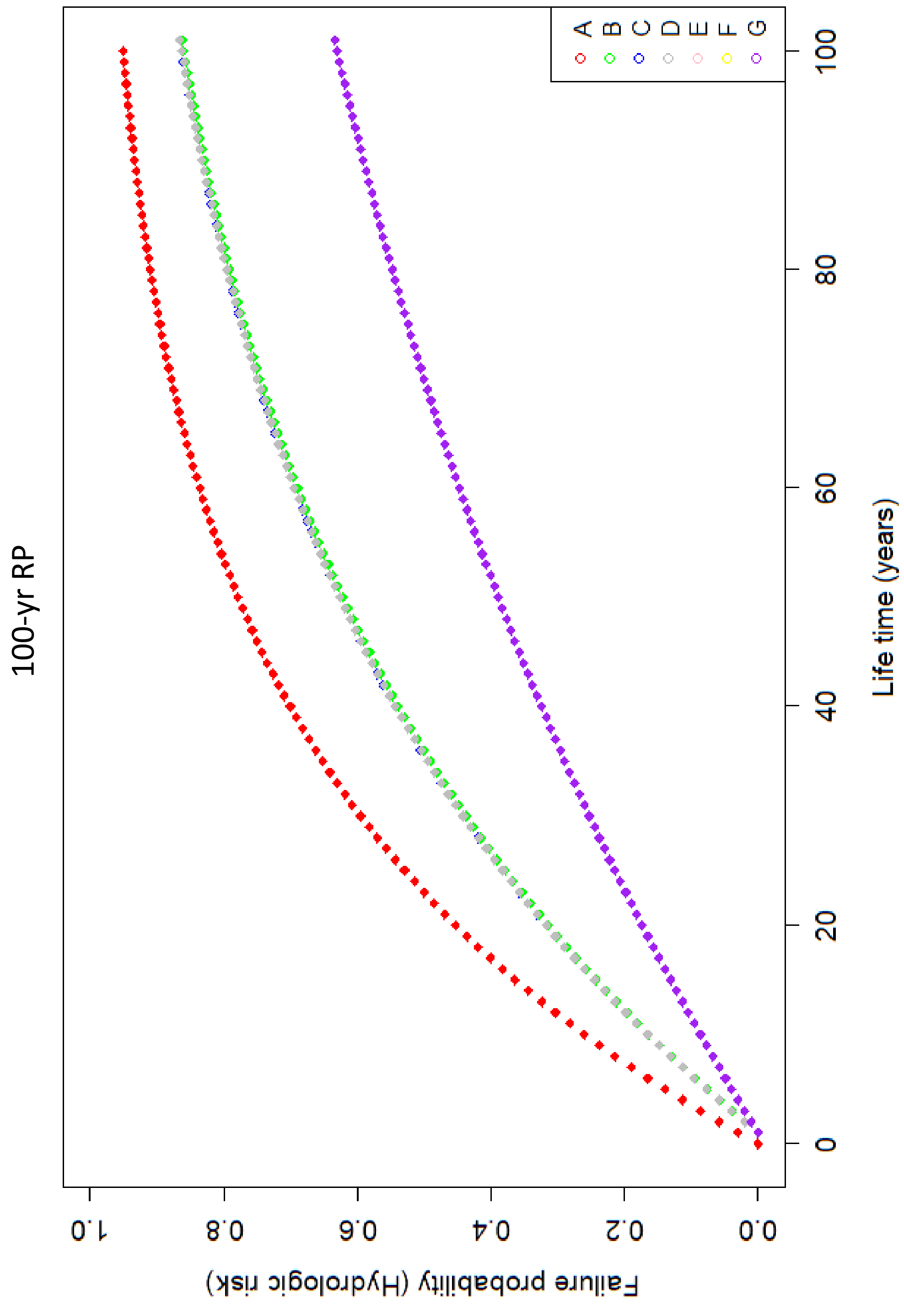

(a)

 doi:10.20944/preprints202210.0167.v1

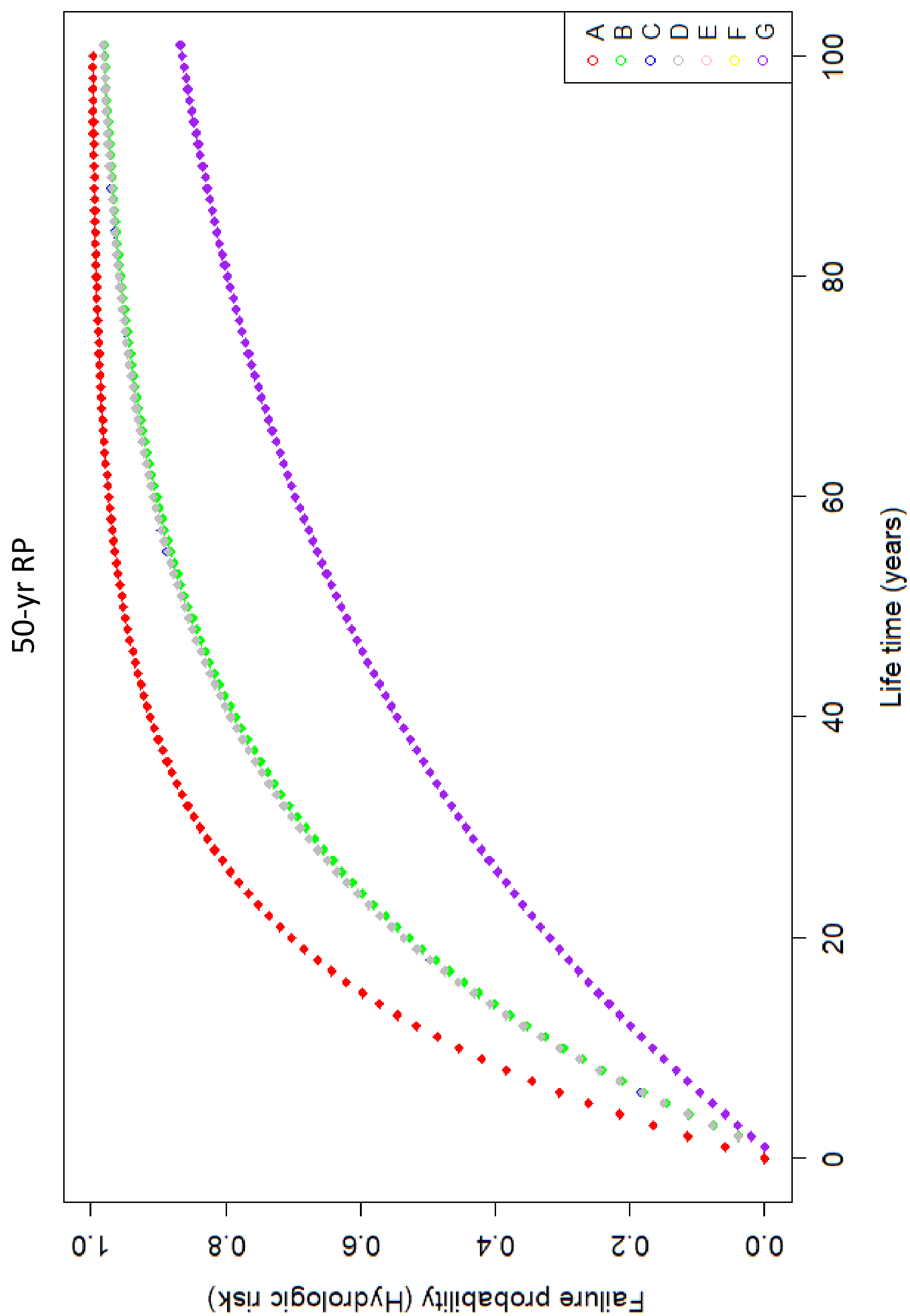

(b)

Preprints (www.preprints.org) | NOT PEER-REVIEWED | Posted: 12 October 2022 doi:10.20944/preprints202210.0167.v1

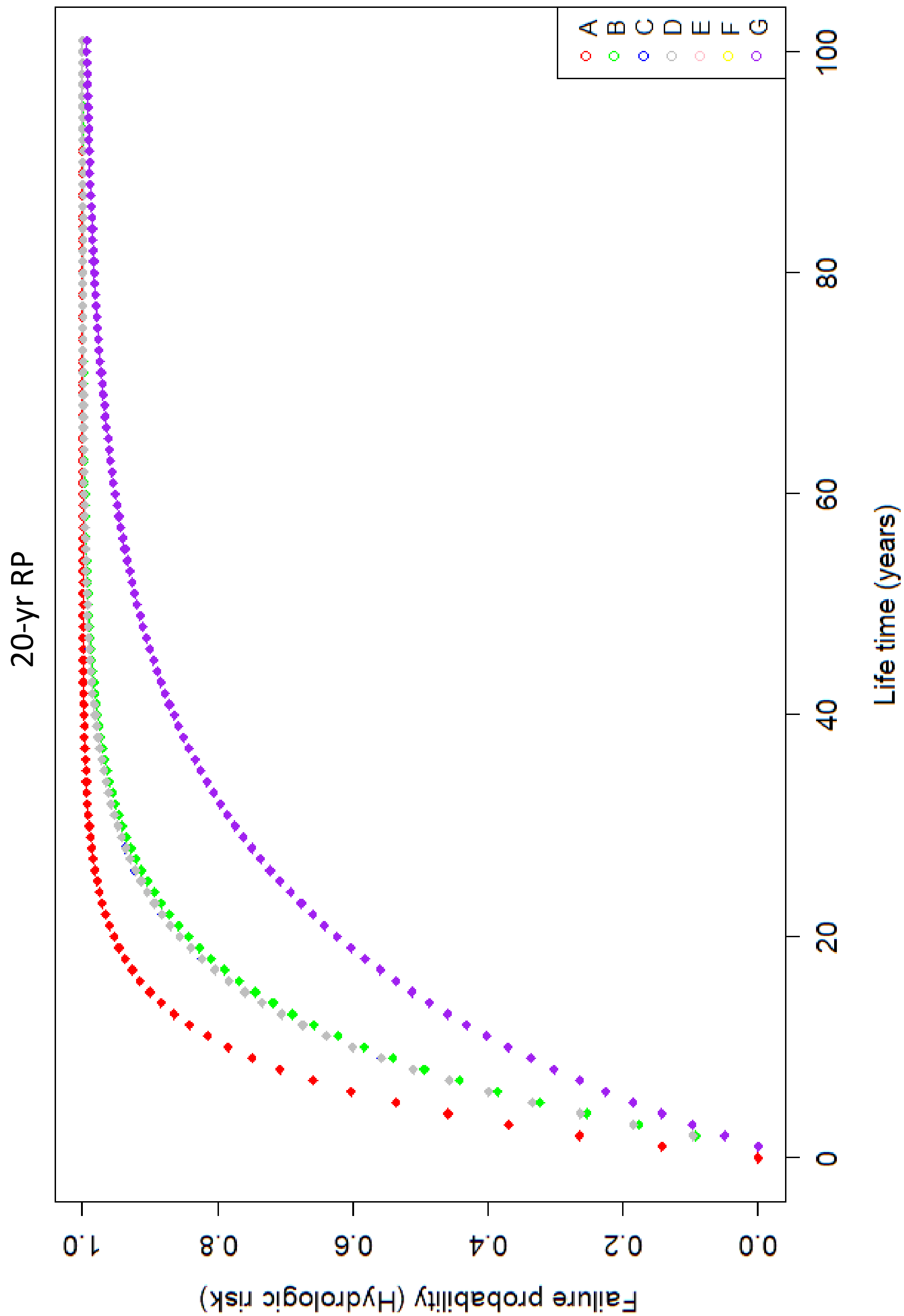

(c)

 doi:10.20944/preprints202210.0167.v1

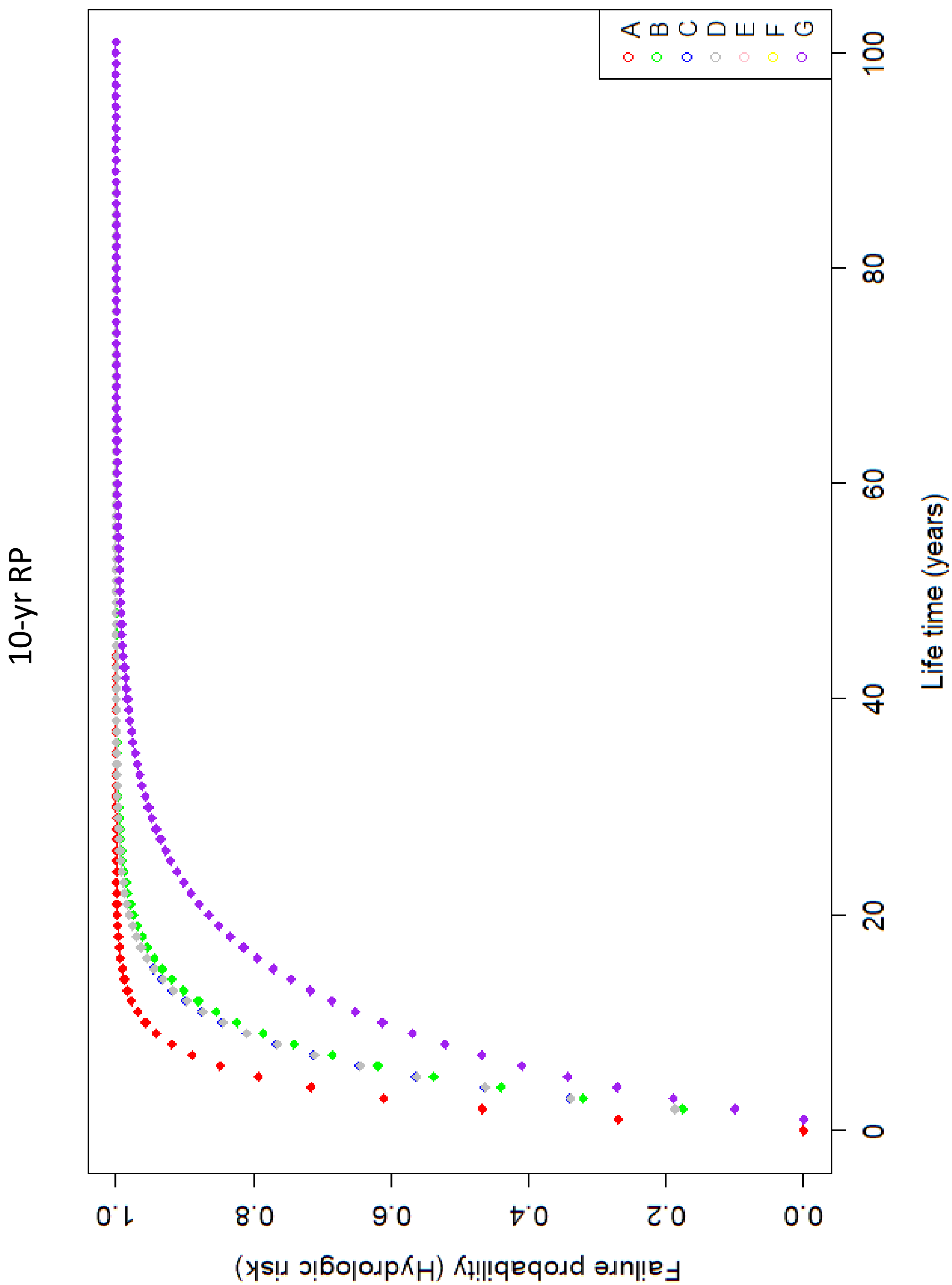

(d)

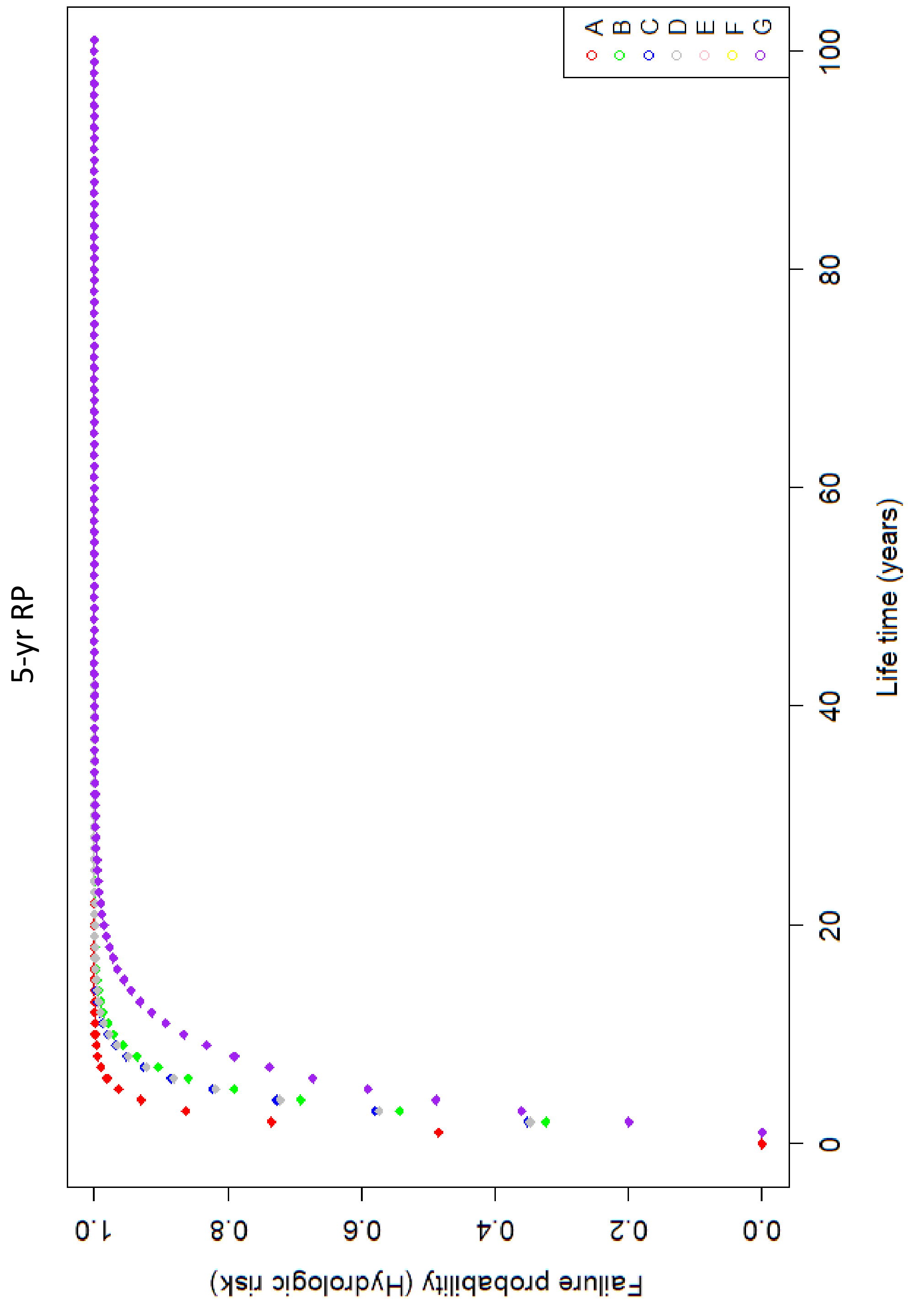

(e)

Figure 3: Assessments in the hydrologic risk of CF events for return periods (RPs) (a) 100 years, (b) 50-years, (c) 20-years (d) 10-years, (e) 5-years [Note: A [red colour]- describing trivariate CF hazard scenario for OR-joint case; B [green colour]- describing bivariate CF hazard scenario between flood pair rainfall and storm surge for OR-joint case; C [blue colour]- describing bivariate CF hazard scenario for flood pair storm

surge and river discharge for OR-joint case; D [grey colour]- describing bivariate CF hazard scenario for flood pair rainfall and river discharge for OR-joint case; E [pink colour]- describing univariate hazard scenario through rainfall events; F [yellow colour] - describing univariate hazard scenario through storm surge events; G [purple colour] - describing univariate hazard scenario through river discharge events]

Abbreviations: CE: Compound Event; CF: Compound Flooding; GOF: Goodness-of-fit; KDE: Kernel Density Estimation; FP: Failure Probability; JRP(s): Joint Return Period(s); PDF(s): Probability Density Function(s); CDF(s): Cumulative Distribution Function(s); JCDF: Joint CDF; FFA: Flood Frequency Analysis; EV: Extreme value; GEV: Generalized Extreme Value; SLR: Sea Level Rise; MSE: Mean Square Error; RMSE: Root Mean Square Error; MAE: Maximum Absolute Error; AIC: Akaike Information Criterion; BIC: Bayesian Information Criterion; HQC: Hannan-Quinn Information Criterion; NSE: Nash- Sutcliffe Model Efficiency; CWL: Coastal Water Level; MLE: Maximum Likelihood Estimation; DPI: Direct Plug-in; AMISE: Asymptotic Mean Integrated Squared Error; MK: Mann-Kendall; CHS: Canadian Hydrographic Service; FNA: Fully Nested Archimedean; PCC: Pair-copula Construction; D-vine: Drawable-vine; Q-Q Plot: Quantile-Quantile Plot; M-K: Mann-Kendall; SNHT: Standard Normal Homogeneity Test; P-P plot: Probability-Probability plot; τ: Kendall's tau; ϱ: Spearman's rho; ROT: Rule of Thumb; CCDFs: Conditional Cumulative Distribution Functions; CvM: Cramer-vin Mises; L-L: Log-likelihood

Author Contributions: Project focus and supervision, S.P.S.; methodology, software, formal analysis, S.L.; writing—original draft preparation, S.L.; writing—review and editing, S.L. and S.P.S.; project administration, S.P.S.; funding acquisition, S.P.S.

Funding: This research was funded by the Natural Sciences and Engineering Research Council of Canada (NSERC) collaborative grant with the Institute for Catastrophic Loss Reduction (ICLR) to the second author [Collaborative Research and Development (CRD) Grant- CRDPJ 472152-14].

Data Availability Statement: Data used in the presented research are available at https://tides.gc.ca/eng/data (CWL data) (accessed on 9 June 2021).; https://wateroffice.ec.gc.ca/search/historical_e.html (Streamflow discharge records) (accessed on 15 June 2021); https://climate.weather.gc.ca/ (rainfall data) (accessed on 22 June 2021).

Acknowledgements: We are thankful for Canada's Fisheries and Ocean assistance for the coastal water level (CWL) data and Environment and Climate Change Canada for daily river discharge data. Special thanks to the Canadian Hydrographic Service (CHS) for providing the tide data. We are special thanks for the funding provided by NSERC (Natural Sciences and Engineering Research Council) and ICLR (Institute for Catastrophic Loss Reduction) in Canada.

Conflicts of Interest: The authors declare no conflict of interest.

References

[1] Seneviratne, S., Nicholls, N., Easterling, D., Goodess, C., Kanae, S., Kossin, J., Luo, Y., Marengo, J., McInnes, K., Rahimi, M., Reichstein, M., Sorteberg, A., Vera, C., and Zhang, X. (2012) Changes in climate extremes and their impacts on the natural physical environment, Manag.

Risk Extrem. Events Disasters to Adv. Clim. Chang. Adapt., 109–230, available at: https://www. ipcc.ch/pdf/special-reports/srex/SREX-Chap3_FINAL.pdf.

[2] Wahl, T., Jain, S., Bender, J., Meyers, S. D., and Luther, M. E. (2015) Increasing risk of compound flooding from storm surge and rainfall for major US cities, Nat. Clim. Change, 5, 1093–1097, https://doi.org/10.1038/nclimate2736.

[3] Hendry, A., Haigh, I. D., Nicholls, R. J., Winter, H., Neal, R., Wahl, T., Joly-Laugel, A., and Darby, S. E. (2019) Assessing the characteristics and drivers of compound flooding events around the U.K. coast, Hydrol. Earth Syst. Sci., 23, 3117–3139, https://doi.org/10.5194/hess-23-3117-2019.

[4] Fritz, H. M., Blount, C. D., Thwin, S., Thu, M. K., and Chan, N (2009). Cyclone Nargis storm surge in Myanmar, Nat. Geosci., 2, 448– 449, https://doi.org/10.1038/ngeo558.

[5] Jonkman, S. N., Maaskant, B., Boyd, E., and Levitan, M. L. (2009). Loss of life caused by the flooding of New Orleans after hurricane Katrina: Analysis of the relationship between flood characteristics and mortality, Risk Anal., 29, 676–698, https://doi.org/10.1111/j.1539-6924.2008.01190.x.

[6] Emanuel, K. (2017). Assessing the present and future probability of Hurricane Harvey's rainfall, P. Natl. Acad. Sci. USA, 114, 12681–12684, https://doi.org/10.1073/pnas.1716222114.

[7] WV Sweet, J Park, From the extreme to the mean: Acceleration and tipping points of coastal inundation from sea level rise. Earths Future 2, 579–600 (2014).

[8] AC Kemp, BP Horton, Contribution of relative sea-level rise to historical hurricane flooding in New York city: Historical hurricane flooding in New York City. J Quat Sci 28, 537–541 (2013).

[9] Moftakhari, H. R., Salvadori, G., Aghakouchak, A., Sanders, B. F. and Matthew, R. A. (2017) Compounding effects of sea level rise and fluvial flooding, Proc. Natl. Acad. Sci., 114(37), 9785–9790, doi:10.1073/pnas.1620325114.

[10] Resio and Westerink, (2008), Modeling the Physics of Storm Surges, Physics Today, 61(9), DOI: 10.1063/1.2982120.

[11] Coles, S. G. (2001), An Introduction to Statistical Modelling of Extreme Values, Springer, London.

[12] Coles, S., J. Heffernan, and J. Tawn (1999), Dependence measures for extreme value analyses, Extremes, 2(4), 339–365.

[13] Svensson, C. and Jones, D. A.: Dependence between extreme sea surge, river flow and precipitation in eastern Britain, Int. J. Climatol., 22, 1149–1168, https://doi.org/10.1002/joc.794, 2002.

[14] Cooley, D., R. A. Davis, and P. Naveau (2010), The pairwise beta distribution: A flexible parametric multivariate model for extremes, J. Multivariate Anal., 101(9), 2103–2117.

[15] Zheng F, Westra S, Sisson S.A (2013) Quantifying the between extreme rainfall and storm surge in the coastal zone. Journal of Hydrology 505: 172-187.

[16] Zheng F, Seth W, Michael L, Sisson SA (2014) Modeling dependence between extreme rainfall and storm surge to estimate coastal flooding risk. Water Resour Res 50(3):2050–2071.

[17] Joe H (1997) Multivariate models and dependence concept. CRC Press, Boca Raton, Fla.

[18] Nelsen R.B. (2006). An introduction to copulas, Springer, New York.

[19] Karmakar S, Simonovic SP (2009) Bivariate flood frequency analysis. Part-2: a copula-based approach with mixed marginal distributions. J Flood Risk Manag 2(1):1–13. https://doi.org/10.1111/j.1753- 318X.2009.01020.x

[20] Latif, S., Mustafa, F. (2020a) Copula-based multivariate flood probability construction: a review. Arab J Geosci 13, 132 https://doi.org/10.1007/s12517-020-5077-6.

[21] Latif S, Mustafa, F. (2020b) A nonparametric copula distribution framework for bivariate joint distribution analysis of flood characteristics for the Kelantan River basin in Malaysia[J]. AIMS Geosciences, 6(2): 171-198. doi: 10.3934/geosci.2020012.

[22] Lian, J. J., Xu, K., and Ma, C. (2013) Joint impact of rainfall and tidal level on flood risk in a coastal city with a complex river network: a case study of Fuzhou City, China, Hydrol. Earth Syst. Sci., 17, 679–689, https://doi.org/10.5194/hess-17-679-2013.

[23] Xu K, Ma C, Lian J, Bin L (2014) Joint probability analysis of extreme precipitation and storm tide in a coastal city under changing environment. PLoS ONE 9(10):e109341–e109341.

[24] Masina, M., Lamberti, A., & Archetti, R. (2015). Coastal flooding: A copula-based approach for estimating the joint probability of water levels and waves. Coastal Engineering, 97, 37–52. doi: 10.1016/j.coastaleng.2014.12.010.

[25] Paprotny, D., Vousdoukas, M. I., Morales-Nápoles, O., Jonkman, S. N., and Feyen, L.: Compound flood potential in Europe, Hydrol. Earth Syst. Sci. Discuss., https://doi.org/10.5194/hess-2018-132, 2018.

[26] Zellou, B., & Rahali, H. (2019). Assessment of the joint impact of extreme rainfall and storm surge on the risk of flooding in a coastal area. Journal of Hydrology, 569, 647–665. doi:10.1016/j.jhydrol.2018.12.028.

[27] Ghanbari, M., Arabi, M., Kao, S., Obeysekera, J., & Sweet, W. (2021). Climate Change and Changes in Compound Coastal-Riverine Flooding Hazard Along the U.S. Coasts. Earth's Future, 9(5). doi:10.1029/2021ef002055.

[28] Serinaldi F, Grimaldi S (2007) Fully nested 3-copula procedure and application on hydrological data. J Hydrol Eng 12(4):420–430. https:// doi.org/10.1061/(ASCE)1084-0699(2007)12:4(420).

[29] Grimaldi S, Serinaldi F (2006) Asymmetric copula in multivariate flood frequency analysis. Adv Water Resour 29:1155–1167. https://doi. org/10.1016/j.advwatres.2005.09.005.

[30] Reddy, M.J.; Ganguli, P. Probabilistic assessments of flood risks using trivariate copulas. Theor. Appl. Climatol. 2013, 111, 341–360.

[31] Kao S, Govindaraju R (2008) Trivariate statistical analysis of extreme rainfall events via the Plackett family copulas. Water Resour Res 44. https://doi.org/10.1029/2007WR006261.

[32] Fan L, Zheng Q (2016) Probabilistic modelling of flood events using the entropy copula. Adv Water Resour 97:233–240. https://doi.org/10. 1016/2Fj.advwatres.2016.09.016.

[33] Genest C, Favre AC, Beliveau J, Jacques C (2007) Metaelliptical copulas and their use in frequency analysis of multivariate hydrological data. Water Resour Res 43:W09401. https://doi.org/10.1029/ 2006WR005275.

[34] Whelan, N. Sampling from Archimedean copulas. Quant. Financ. 2004, 4, 339–352.

[35] Savu, C.; Trede, M. Hierarchies of Archimedean copulas. Quant Financ. 2010, 10, 95–304.

[36] Hofert, M.; Pham, D. Densities of nested Archimedean copulas. J. Multivar. Anal. 2013, 118, 37–52.

[37] Bedford, T.; Cook, R.M. Vines-a new graphical model for dependent random variables. Ann. Stat. 2002, 30, 1031–1068

[38] Aas, K.; Berg, D. Models for construction of multivariate dependence—A comparison study. Eur. J. Financ. 2009, 15, 639–659.

[39] Aas, K.; Czado, K.C.; Frigessi, A.; Bakken, H. Pair-copula constructions of multiple dependence. Insur. Math. Econ. 2009, 44, 182–198.

[40] Graler B, Berg M.J.V., Vandenberg S, Petroselli A, Grimaldi S, Baets BD, Verhost N.E.C. (2013) Multivariate return periods in hydrology: a critical and practical review focusing on synthetic design hydrograph estimation. Hydrol Earth Sys Sci 17:1281–1296. https://doi.org/10.5194/hess-17-1281-2013.

[41] Bevacqua E, Maraun D, Hobæk Haff I, Widmann M, Vrac M (2017) Multivariate statistical modelling of compound events via pair-copula constructions: analysis of floods in Ravenna (Italy). Hydrology Earth System Sciences, 21, 2701-2723.

[42] Jane, R., Cadavid, L., Obeysekera, J., & Wahl, T. (2020). Multivariate statistical modelling of the drivers of compound flood events in South Florida. Natural Hazards and Earth System Sciences Discussions, 1– 30.

[43] Saghafian B, Mehdikhani H (2014) Drought characteristics using new copula-based trivariate approach. Nat Hazards 72:1391–1407. https://doi.org/10.1007/s11069-013-0921-6.

[44] Tosunoglu, F., Gürbüz, F. & İspirli, M.N. Multivariate modeling of flood characteristics using Vine copulas. Environ Earth Sci 79, 459 (2020). https://doi.org/10.1007/s12665-020-09199-6

[45] Latif, S., & Mustafa, F. (2020c). Parametric vine copula construction for flood analysis for Kelantan River basin in Malaysia. Civil Engineering Journal, 6(8), 1470-1491.

[46] Silverman B. W. 1986 Density Estimation for Statistics and Data Analysis, 1st edn. Chapman and Hall, London.

[47] Moon Y.-I. Lall U. 1994 Kernel function estimator for flood frequency analysis. Water Resour. Res. 30 (11), 3095–3103.

[48] Sharma A. Lall U. Tarboton D. G. 1998 Kernel bandwidth selection for a first order nonparametric streamflow simulation model. Stoch. Hydrol. Hydraul. 12, 33–52.

[49] Kim T. W. Valdes J. B. Yoo C. 2006 Nonparametric approach for bivariate drought characterization using Palmer drought index. J. Hydrol. Eng. 11 (2), 134–143.

[50] Karmakar S, Simonovic SP (2008) Bivariate food frequency analysis. Part-1: determination of marginal by parametric and nonparametric techniques. J Flood Risk Manag 1:190–200.

[51] Charpentier A, Fermanian J, Scaillet O (2006) Copulas: from theory to application in finance, 1st edn, Risk Books, Torquay, U.K., chap The Estimation of Copulas: Theory and Practice.

[52] Rauf, U.F.A., Zeephongsekul, P. Analysis of Rainfall Severity and Duration in Victoria, Australia using Nonparametric Copulas and Marginal Distributions. Water Resour Manage 28, 4835–4856 (2014). https://doi.org/10.1007/s11269-014-0779-8.

[53] Harrell FE, Davis CE (1982) A new distribution-free quantile estimator. Biometrika 69(3):635–640.

[54] Chen SX (1999) Beta kernel estimators for density functions. Comput Stat Data Anal 31(2):131–145.

[55] Pfeifer, D., Strassburger, D. and Philipps, J (2009): "Modelling and simulation of dependence structures in nonlife insurance with Bernstein copulas," Working Paper, Carl von Ossietzky University, Oldenburg.

[56] SANCETTA, A. AND S. SATCHELL (2004): "The Bernstein copula and its applications tomodeling and approximations of multivariate distributions," Econometric Theory, 20, 1–38.

[57] Weiss, G. N. F., & Scheffer, M. (2012). Smooth Nonparametric Bernstein Vine Copulas. SSRN Electronic Journal. doi:10.2139/ssrn.2154458

[58] KULPA, T. (1999): "On approximation of copulas," International Journal of Mathematics and Mathematical Sciences, 22, 259–269.

[59] Latif, S., Simonovic, S.P. (2022a). Nonparametric approach to copula estimation in compounding the joint impact of storm surge and rainfall events in coastal flood analysis, 16 August 2022, PREPRINT (Version 1) available at Research Square [https://doi.org/10.21203/rs.3.rs-1939067/v1][Accepted for publication].

[60] Pirani, F.J. and Najafi M.R. (2020). Recent trends in individual and multivariate flood drivers in Canada's Coasts. Water Resour Res 56(8). https://doi.org/10.1029/2020WR027785..

[61] Atkinson, D.E., Forbes, D.L. and James, T.S. (2016): Dynamic coasts in a changing climate; in Canada's Marine Coasts in a Changing Climate, (ed.) D.S. Lemmen, F.J. Warren, T.S. James and C.S.L. Mercer Clarke; Government of Canada, Ottawa, Ontario, p. 27-68.

[62] Wand, M. P., J. S. Marron and D. Ruppert, (1991), "Transformations in Density Estimation: Rejoinder (in Theory and Methods)", Journal of the American Statistical Association, 86, pp 360–361.

[63] Müller, H. G., 1991, "Smooth Optimum Kernel Estimators near Endpoints", Biometrika, 78, pp 521–530.

[64] Schuster, E., (1985), "Incorporating Support Constraints into Nonparametric Estimators of Densities", Communications in Statistics: Theory and Methods, 14, pp 1123–1136

[65] Brown BM, Chen SX (1999) Beta-bernstein smoothing for regression curves with compact support. Scand J Stat 26(1):47–59.

[66] Chen, S. X., (2000), "Beta Kernel for Regression Curve", Statistica Sinica, 10, pp 73–92.

[67] Bouezmarni, T. and J. M. Rolin, 2003, “Bernstein Estimator for Unbounded Density Function”, Université Catholique de Louvain-la-Neuve.

[68] Nagler T (2014). Kernel Methods for Vine Copula Estimation. Master’s thesis, Technische Universität München.

[69] Lorentz, G. (1953). Bernstein Polynomials. University of Toronto Press.

[70] Tenbusch, A. (1994). Two-dimensional Bernstein polynomial density estimation. Metrika 41, 233–253.

[71] DIERS, D., M. ELING, AND S. MAREK (2012): "Dependence modeling in non-life insurance using the Bernstein copula," Insurance: Mathematics and Economics, 50, 430–436.

[72] Bouezmarni, T., Ghouch, E., & Taamouti, A. (2013). Bernstein estimator for unbounded copula densities. Statistics & Risk Modeling, 30(4), 343–360. https://doi.org/10.1524/strm.2013.2003

[73] Santhosh D. Srinivas V. 2013 Bivariate frequency analysis of flood using a diffusion kernel density estimator. Water Resour. Res. 49, 8328–8343.

[74] Latif, S and Mustafa, F. (2020c) "A nonparametric statistical framework using a kernel density estimator to approximate flood marginal distributions – a case study for the Kelantan River Basin in Malaysia." Water supply 20: 1509-1533.

[75] Jones M. C. Marron J. S. Sheather S. J. 1996 A brief survey of bandwidth selection for density estimation. J. Am. Stat. Assoc. 91, 401–407.

[76] Sheather, S. J. and Jones, M. C. (1991). A reliable data-based bandwidth selection method for kernel density estimation. Journal of the Royal Statistical Society, Series B, 53, 683–690.

[77] Wand, M. P. & Jones, M. C. (1995) Kernel Smoothing. Chapman and Hall, London, UK.

[78] Chen, S. (2015). Optimal Bandwidth Selection for Kernel Density Functionals Estimation. Journal of Probability and Statistics, 2015, 1–21. doi:10.1155/2015/242683.

[79] Czado, C.; Jeske, S.; Hofmann, M. Selection strategies for regular vine copulae. J. French Society Stat. 2013, 154, 174–190.

[80] Kurowicka, D.; Cooke, R. Uncertainty Analysis with High Dimensional Dependence Modelling; John Wiley: Hoboken, NJ, U.S.A., 2006.

[81] Vernieuwe H, Vandenberghe S, Baets BD, Verhost N.E.C. (2015) A continuous rainfall model based on vine copulas. Hydrol Earth Syst Sci 19:2685–2699. https://doi.org/10.5194/hess-19-2685-2015.

[82] Latif, S, and Simonovic, S.P. (2022b). Compounding joint impact of rainfall, storm surge and river discharge on coastal flood risk: An approach based on 3D Fully Nested Archimedean Copulas, 13 April 2022, PREPRINT (Version 1) available at Research Square [https://doi.org/10.21203/rs.3.rs-1452437/v1].

[83] Yue S, Rasmussen P (2002) Bivariate frequency analysis: discussion of some useful concepts in hydrological applications. Hydrol Process 16:2881–2898.

[84] Shiau JT (2003) Return period of bivariate distributed hydrological events. Stoch Environ Res Risk Assess 17(1–2):42–57. https://doi.org/10.1007/s00477-003-0125-9.

[85] Salvadori G (2004) Bivariate return periods via-2 copulas. J Royal Stat Soc Series B 1:129–144. https://doi.org/10.1016/j.stamet.2004.07.002.

[86] Salvadori G, De Michele C (2004) Frequency analysis via copulas: theoretical aspects and applications to hydrological events. Water Resour Res 40:W12511. https://doi.org/10.1029/2004WR003133.

[87] Zhang L, Singh VP (2007) Trivariate flood frequency analysis using the Gumbel-Hougaard copula. J Hydrol Eng 12(4):431–439. https://doi. org/10.1061/(ASCE)1084-0699(2007)12:4(431).

[88] Zhang L, Singh VP (2006) Bivariate flood frequency analysis using copula method. J Hydrol Eng 11(2):150. https://doi.org/10.1061/(ASCE)1084-0699(2006)11:2(150).

[89] Reddy MJ, Ganguli P (2012) Bivariate flood frequency analysis of Upper Godavari River flows using Archimedean copulas. Water Resour Manage: DOI. https://doi.org/10.1007/s11269-012-0124-z.

[90] Requena A, Flores I, Mediero L, Garrote L (2016) Extension of observed flood series by combining a distributed hydro-meteorological model and a copula based model. Stoch Environ Res Risk Assess 30(5). https://doi.org/10.1007/s00477-015-1138-x

[91] Mann HB (1945) Nonparametric test against trend. Econometrics 13:245–259.

[92] Kendall MG (1975) Rank correlation methods, 4th edn. Charles Griffn, London, p 1975.

[93] Pettitt, A.N. A Non-Parametric Approach to the Change-Point Problem. Appl. Stat. 1979, 28, 126–135.

[94] Alexanderson, H. A homogeneity test applied to precipitation data. J. Clim. 1986, 6, 661–675.

[95] Buishand, T.A. Some methods for testing the homogeneity of rainfall records. J. Hydrol. 1982, 58, 11–27.

[96] Gringorten II (1963) A plotting rule of extreme probability paper. J Geophys Res 68(3):813–814.

[97] Moriasi, D.N., Arnold, J.G., Van Liew, M.W., Bingner, R.L., Harmel, R.D. and Veith, T.L. (2007), "Model evaluation guidelines for systematic quantification of accuracy in watershed simulations", Transactions of the ASABE, 50(3), 885- 900.

[98] Akaike, H. (1974). "A new look at the statistical model identification", IEEE T. Automat. Contr., 19(6), 716-723.

[99] Schwarz, G.E. (1978), "Estimating the dimension of a model", Ann. Stat., 6(2), 461e464.

[100] Hannan, E. J., and B. G. Quinn (1979), "The Determination of the order of an autoregression", Journal of the Royal Statistical Society, Series B, 41: 190–195.

[101] Willmott, C. and Matsuura, K. (2005), "Advantage of the Mean Absolute Error (M.A.E.) OVER THE Root Mean Square Error (RMSE) in assessing average model performance", Clim. Res., 30, 79-82.

[102] Farrel, P.J. and Stewart, K.R. (2006), "Comprehensive study of tests for normality and symmetry: Extending the Spiegelhalter test", J. Stat. Comput. Simul., 76, 803-816. https://doi.org/10.1080/10629360500109023.

[103] Nash, J. and Sutcliffe, J. (1970), "River flow forecasting through conceptual models part i e a discussion of principles", J. Hydrol., 10(3), 282e290.

[104] R Core Team (2021). R: A language and environment for statistical computing. R Foundation for Statistical Computing, Vienna, Austria. URL https://www.R-project.org/.

[105] Nagler, T. (2018) kdecopula: An R Package for the Kernel Estimation of Bivariate Copula Densities. Journal of Statistical Software 84(7), 1-22.

[106] Nagler, T., Czado, C. (2016) Evading the curse of dimensionality in nonparametric density estimation with simplified vine copulas. Journal of Multivariate Analysis 151, 69-89 (doi: 10.1016/j.jmva.2016.07.003).

[107] De Michele C, Salvadori G, Canossi M, Petaccia A, Rosso R (2005) Bivariate statistical approach to check the adequacy of dam spillway. J Hydrol Eng 10(1):50–57.

[108] Klein B, Pahlow M, Hundecha Y, Schumann A (2010) Probability analysis of hydrological loads for the design of food control system using copulas. J Hydrol Eng ASCE 15:360–369.

[109] Genest C, Rémillard B (2008) Validity of the parametric bootstrap for goodness-of-ft testing in semiparametric models. Ann l'Inst Henri Poincare Prob Stat 44:1096–1127.

[110] Genest C, Rémillard B, Beaudoin D (2009) Goodness-of-ft tests for copulas: a review and a power study. Insur Math Econ 44:199–214.

[111] Read, L.K., Vogel, R.M. (2015) Reliability, Return Periods, and Risk Under Nonstationarity." Water Resources Research 51, no. 8:6381–6398. doi:10.1002/2015wr017089

[112] Salvadori, G., F. Durante, C. De Michele, M. Bernardi, and L. Petrella. (2016). A Multivariate Copula-Based Framework for Dealing with Hazard Scenarios and Failure Probabilities." Water Resources Research 52(5): 3701–3721. doi:10.1002/2015wr017225

[113] Serinaldi, F. Dismissing return periods! Stoch. Hydrol. Hydraul. 2014, 29, 1179–1189.

[114] Xu, Y.; Huang, G.; Fan, Y. Multivariate flood risk analysis for Wei River. Stoch. Hydrol. Hydraul. 2015, 31, 225–242.